Technical Report

TR-10-32

Stress-strain relation of bentonite at undrained shear

Laboratory tests to investigate the influence of material composition and test technique

Ann Dueck, Lennart Börgesson, Lars-Erik Johannesson
Clay Technology AB

December 2010

Svensk Kärnbränslehantering AB
Swedish Nuclear Fuel
and Waste Management Co

Box 250, SE-101 24 Stockholm
Phone +46 8 459 84 00

ISSN 1404-0344
SKB TR-10-32

Stress-strain relation of bentonite at undrained shear

Laboratory tests to investigate the influence of material composition and test technique

Ann Dueck, Lennart Börgesson, Lars-Erik Johannesson
Clay Technology AB

December 2010

Keywords: SKBdoc 1223371, Bentonite, Shear rate, Swelling pressure, Triaxial test, Unconfined compression test, Undrained shear strength.

Abstract

This report describes a laboratory study conducted to update the material model of the buffer material used in the analyses of the effect of a rock shear through a deposition hole. The study considers some new conditions and is especially focused on the reference case with MX-80Ca developed for SR-Site (MX-80 ion exchanged to Ca). The material model is based on relations between density, swelling pressure, shear strength and rate of strain. The reference model is described by Börgesson et al. (2010).

The laboratory study is focused on undrained stress-strain-strength properties, which have been studied mainly by conducting triaxial tests and unconfined compression tests. The test results are compared to the earlier measurements and models which show that the new results fit very well into the general picture and models. For the new conditions suitable values of constants included in the model are proposed.

Sammanfattning

Denna rapport beskriver en laboratoriestudie som utförts för att uppdatera den materialmodell för buffertmaterial som används i analysen av effekten av en bergskjuvning genom ett deponeringshål. Studien beaktar några nya förhållanden och är speciellt inriktad på referensfallet med MX-80Ca som tagits fram för SR-Site (MX-80 jonbytt till Ca). Materialmodellen är baserad på relationerna mellan densitet, svälltryck, skjuvhållfasthet och töjningshastighet. Referensmodellen beskrivs av Börgesson et al. (2010).

Inriktningen på laboratoriestudien har varit spänning-töjning-hållfasthets egenskaper under odränerade förhållanden vilket har undersökts genom att utföra triaxialförsök och enaxiella tryckförsök. Försöksresultaten har jämförts med tidigare mätningar och modeller och de nya mätningarna stämmer överens med den generella bilden och modellerna. För de nya villkor som undersökts har lämpliga värden på konstanter som ingår i modellen föreslagits.

Contents

1 Introduction

1.1 Background

This report describes a laboratory study conducted to update the material model of the buffer material used in the analyses of the effect of a rock shear through a deposition hole. The study considers some new conditions and is especially focused on the reference case with MX-80Ca developed for SR-Site (MX-80 ion exchanged to Ca).

The general model mainly describing the relation between density, swelling pressure, shear strength and rate of strain for different bentonites has been developed and reported by Börgesson et al. (1995, 2004). The model has been and will be used for calculating stresses and strains in the buffer at different types of shear load (Börgesson and Hernelind 2006, Hernelind 2010).

The model has been continuously updated and the laboratory tests conducted in this study will be used to further update the model regarding mainly two questions which are mentioned below.

This report serves as a presentation of data which is further evaluated and analyzed by Börgesson et al. (2010).

1.2 Objective of the laboratory study

This study of the undrained stress-strain-strength properties of buffer material has been focused on the impact of

- exposure to high pore water pressure,
- change of the dominating exchangeable ions,
- influence of strain rate.

The effect of increasing pore water pressure and its relationship to total stress and swelling pressure in bentonite was investigated by Harrington and Birchall (2007). The results showed significant hysteresis between ascending and descending the pore water pressure. In one of the tests the swelling pressure increased from the initial value 7.2 MPa to 14.4 MPa after exposure to a pore water pressure of 46 MPa. Another specimen was exposed to a pore water pressure of 37 MPa and the swelling pressure then increased from 5.1 MPa to 8.4 MPa (Harrington 2008, pers. comm.). In the present report the implication of this behaviour on the shear strength has been studied.

Influence of the dominating ions of different bentonites on sealing properties has been extensively investigated by Karnland et al. (2006). In the present report the implication of this behaviour on the stress-strain-strength properties has been studied.

A rock shear caused by an earthquake yield a very fast rock displacement and the stress-strain behaviour of bentonite is rate dependent. New tests at fast shear have been performed and a revised model for the influence of strain rate is suggested.

1.3 Materials tested

The following three types of bentonite have been tested:

- MX-80 including specimens previously exposed to very high pore water pressure,
- Deponit CaN, which is a Ca dominated bentonite,
- MX-80Ca and MX-80Na, which are MX-80 ion-exchanged to Ca and Na respectively.

Properties regarding mineralogy and sealing properties of the sodium dominated MX-80 (Wyoming bentonite product from American Colloid Co.) and the calcium dominated Deponit CaN (bentonite from Milos with the commercial name including IBECO) are reported by Karnland et al. (2006).

2 Test techniques

2.1 General

The strength of bentonite is much dependent on the swelling pressure, which in turn depends on the density, so the main tests performed in this study were swelling pressure tests, triaxial tests and unconfined compression tests. For some material the relative humidity was measured above the dismantled specimen and the corresponding suction was calculated and used as a measure of the swelling pressure.

In this chapter the test methods and some related terms are described.

2.2 Water content and bulk density determination

The base variables water content w (%), void ratio e and degree of saturation S_r (%) were determined according to Equations 2-1 to 2-3.

$$w = 100 \cdot \frac{m_{tot} - m_s}{m_s} \tag{2-1}$$

$$e = \frac{\rho_s}{\rho}(1 + w/100) - 1 \tag{2-2}$$

$$S_r = \frac{\rho_s \cdot w}{\rho_w \cdot e} \tag{2-3}$$

Where

m_{tot} = total mass of the specimen (g)

m_s = dry mass of the specimen (g)

ρ_s = particle density (kg/m^3)

ρ_w = density of water (kg/m^3)

ρ = bulk density of the specimen (kg/m^3)

The dry mass of the specimen was obtained from drying the wet specimen at 105˚C for 24h. The bulk density was calculated from the total mass of the specimen and the volume determined by weighing the specimen above and submerged into paraffin oil.

2.3 Ion exchange of MX-80

One type of bentonite tested in this study was the ion exchanged MX-80, denominated MX-80Ca and MX-80Na. Compacted specimens of MX-80 were placed in a saturation device with filters on both sides. De-ionized water was applied to the filters after evacuation of filters and tubes. The specimens were saturated at constant volume conditions. After a couple of days the de-ionized water was changed to a chloride solution circulating through the filters above and below the specimens. The cation of the chloride solution was the same as the desired dominating cation of the clay (i.e. Na^+ or Ca^{2+}). Solutions of NaCl or $CaCl_2$ were used. The method is further described in Appendix 1.

The method used is based on a description by Karnland et al. (2006) where purified and ion-exchanged material was produced. However, in that description all accessory minerals were also removed which was not the case in the ion exchange used in this present study described above.

2.4 Relative humidity

The relative humidity *RH* (%) was measured by capacitive sensors. The sensors were calibrated above saturated salt solutions being attached to a calibration device. The same device was also used for the measurement of *RH* of the buffer samples with the salt solution used for the calibration exchanged for the actual sample.

The relative humidity is defined according to Equation 2-4. From the relative humidity the corresponding suction ψ (kPa) can be determined according to the thermodynamic equation, Equation 2-5, given by e.g. Fredlund and Rahardjo (1993).

$$RH = 100 \cdot \frac{p}{p_s} \tag{2-4}$$

where

p = partial pressure of pore-water vapour (kPa)

p_s = saturation pressure of water vapour over a flat surface of pure water at the same temperature (kPa)

$$\psi = -\frac{R \cdot T}{v_{w0} \cdot \omega_v} \ln\left(\frac{p}{p_s}\right) \tag{2-5}$$

where

T = absolute temperature (K)

R = universal gas constant (8.31432 J/(mol K))

v_{w0} = specific volume of water ($1/\rho_w$ m^3/kg)

ω_v = molecular mass of water vapour (18 kg/kmol)

RH measurements or calculated suction values can be used as a measure of the swelling pressure. Correspondence between water retention properties in terms of chemical potential, *RH* or suction and swelling pressure under certain conditions has previously been shown by e.g. Kahr et al. (1990), Karnland et al. (2005) and Dueck and Börgesson (2007).

When a chloride solution is used as pore water this has to be taken into account in the calculation of suction or swelling pressure. The saturation pressure p_s in Equation 2-5 should then be exchanged for p_e – the vapour pressure set by the chloride solution, to be in accordance with Karnland et al. (2005).

2.5 Swelling pressure

The swelling pressure can be determined in several ways but is with advantage determined in the swelling pressure device used which is described below.

2.5.1 Equipment

The swelling pressure device consists of a steel ring surrounding the specimen having filters on both sides. A piston and a load cell were placed vertically, in the axial direction, above the specimen. The bottom plate and a plate above the load cell were bolted together to keep the volume of the specimen constant. The small deformation required by the load cell for measuring the load was admitted by the movable piston.

2.5.2 Preparation of specimen

Cylindrical specimens were prepared either from blocks by mechanical trimming or by use of a special compaction device where powder was compacted to a certain density. The dimension of the specimens was a diameter of 35 mm and a height between 13 mm and 20 mm.

2.5.3 Test procedure

De-ionized water was applied to the filters after evacuating of air from the filters and the tubes. The specimens had free access to water during the entire testing time. After the test the water was evacuated from the filters and tubes and the water content and the density of the specimen were determined.

2.6 Triaxial test

The stress-strain-strength properties of soil materials are preferably evaluated from triaxial tests. A description concerning technique and evaluation is given by Börgesson et al. (1995).

2.6.1 Equipment

A high pressure triaxial cell was used for all tests. The cell was equipped with standard deformation transducer, load cell and pore- and cell-pressure transducers according to Figure 2-1.

2.6.2 Preparation of specimen

Different preparations were used for the MX-80 specimens, the Deponit CaN specimens and the ion exchanged specimens. For all materials the dimension of the specimens mounted into the triaxial cell was the same; 35 mm in diameter and 70 mm in height.

Three triaxial tests were made on MX-80. Two of those specimens were derived from a block also used by Harrington and Birchall (2007) and one specimen was prepared in the laboratory. The latter specimen was compacted with high water content directly to the correct dimensions and to almost full saturation For the other two tests, cylindrical specimens were prepared by sawing rough work pieces, which were trimmed to a cylindrical form having a diameter of 35 mm and a height of 70 mm.

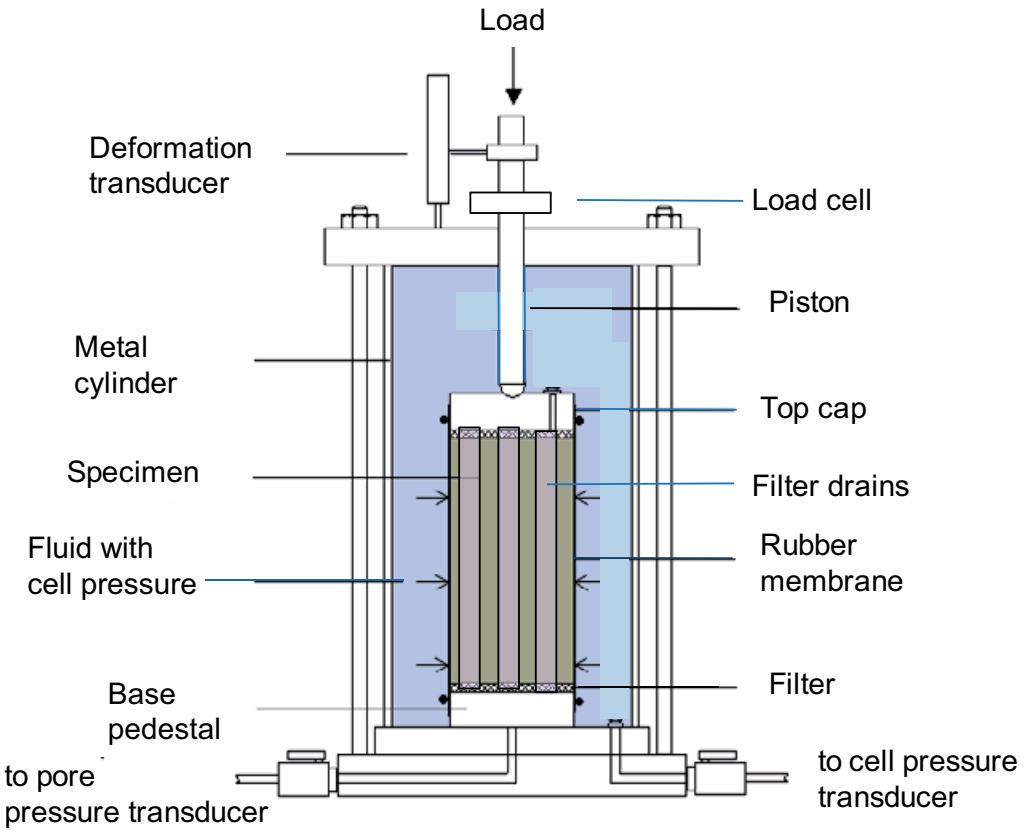

Figure 2-1. *Triaxial test equipment.*

The Deponit CaN specimens were each prepared by compaction of three cylindrical specimens, which on top of each other gave the final height of 70 mm. The specimens were placed in a saturation device with radial saturation and possibility to measure the swelling pressure, axially, during the saturation.

The ion exchanged materials, MX-80Ca and MX-80Na, were each compacted in eight pieces. Each piece was placed in the special device for the ion exchange where the saturation and ion exchange took place, see Appendix 1. After the preparation seven of the pieces were placed on top of each other to have the final height of 70 mm.

The in these ways prepared specimens with the diameter of 35 mm and height of 70 mm were mounted in the triaxial cell and a cell pressure corresponding to an estimate of the actual swelling pressure was applied in the cell. The valves to the pedestal and top-cap were kept closed during an equilibration period and the pore pressure at the base pedestal was measured. Filter paper drains along the specimens were used to accelerate the equalization of the pore pressure.

2.6.3 Test procedure

The cell was placed in a mechanical press when pressure equilibrium was reached. A constant shear rate of $4–9 \cdot 10^{-6}$ mm/s ($6–13 \cdot 10^{-6}$ %/s) was used. The specimen was undrained during the course of shearing. After failure the water content and density of the specimens were determined.

2.6.4 Test results

The cell pressure σ_3 (kPa), pore pressure u (kPa), deformation Δl (mm), and axial force F (kN) were measured during the test. Since the specimens were undrained during shearing no volume change was taken into account. The deviator stress q (kPa) is calculated from Equation 2-6.

$$q = \frac{F}{A_0}\left(\frac{l_0 - \Delta l}{l_0}\right) \tag{2-6}$$

where A_0 is the specimen initial cross section area and l_0 the initial length of the sample. The vertical total stress σ_1 (kPa) is derived from Equation 2-7.

$$\sigma_1 = q + \sigma_3 \tag{2-7}$$

The average effective stress p' (kPa) is derived from Equation 2-8.

$$p' = \frac{1}{3}(\sigma_1 + 2\sigma_3 - 3u) \tag{2-8}$$

The strain ε (%) is derived from Equation 2-9.

$$\varepsilon = \frac{\Delta l}{l_0} \cdot 100 \tag{2-9}$$

2.7 Unconfined compression test

The shear strength can be determined by the unconfined compression test. This technique is much simpler than triaxial tests and should according to the effective stress theory yield the same results but has no control of the pore pressure. In this kind of test a sample is compressed axially with a constant rate of strain with no radial confinement or external radial stress. The test can be regarded as a consolidated unconfined compression test, since the fully water saturated samples are attained by a negative pore pressure, which is similar to the swelling pressure. Results from unconfined compression tests on saturated bentonite have earlier also been reported by Börgesson et al. (2004).

The test type has also been used to quantify relative changes in physical properties between buffer materials exposed to special conditions by Karnland et al. (2009). Since only a relative change between specimens were considered a deviating dimension, with the height equal to the diameter, was used for those tests.

2.7.1 Equipment

The specimen was placed in a mechanical press where a constant rate of deformation was applied to the specimen, Figure 2-2. During the test the deformation and the applied force were measured by means of a load cell and a deformation transducer.

2.7.2 Preparation of specimen

Cylindrical specimens were prepared for the tests and different preparation techniques were used.

Most of the specimens were compacted in a compaction device from powder to specimens with a height and diameter of 20 mm. These specimens were then saturated in a special designed saturation device where de-ionized water was applied after evacuating of air from the filters and the tubes used.

Some specimens were compacted in the compaction device to almost fully saturated specimens having a height and diameter of 20 mm. The powder used for these specimens was mixed with de-ionized water to high initial water content. Finally, a few specimens were prepared from blocks by drilling and trimming cylindrical specimens, 20 mm in diameter and 40 mm in height.

Almost all tests were carried out on specimens having a height equal to twice the diameter, i.e. 40 mm. Since most of the prepared specimens had the height 20 mm two such specimens were used for each test.

2.7.3 Test procedure

The specimens were placed in a mechanical press and the compression started and continued at a constant rate. The normally applied strain rate was 0.01%/s, which means 0.005 mm/s and 0.003 mm/s for the specimen height 40 mm and 20 mm, respectively. Another very fast precision compression machine was used for share rates between 0.1 mm/s and 300 mm/s. After failure the water content and density were determined.

2.7.4 Test results

The specimens were considered as undrained during shearing and no volume change was taken into account. The deviator stress is derived from Equation 2-6.

Initial problems with the contact surface were corrected for. This was done by decreasing the strain with the intercept on the x-axis of a tangent to the stress-strain curve at 500 kPa.

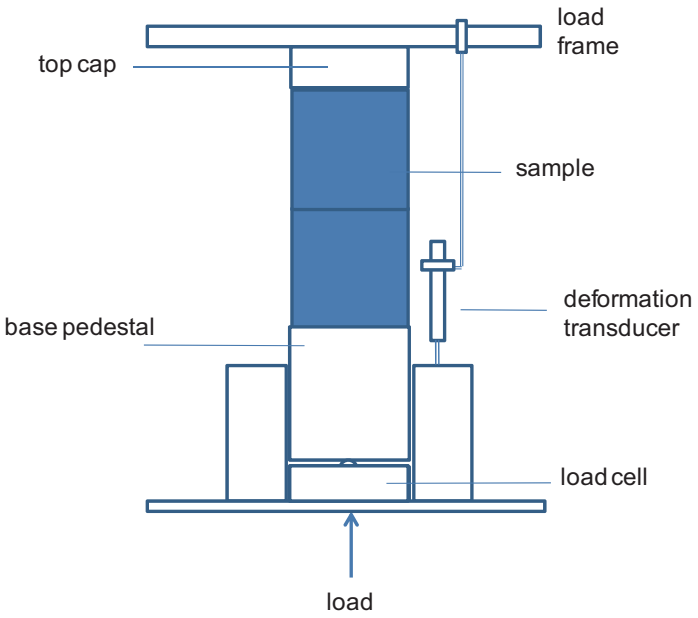

Figure 2-2. *Set-up for the unconfined compression test.*

3 Test results

3.1 General

Three types of bentonite were tested; MX-80, Deponit CaN and ion exchanged MX-80, denominated MX-80Ca and MX-80Na. The latter type of bentonite included in this present study is the ion exchanged MX-80, which was prepared according to Appendix 1. All tests carried out are shown in the test matrix in Appendix 8.

In the test results the legends of each test contain the following final letters denoting the test type used: SP – swelling pressure test, T – triaxial test and UC – unconfined compression test.

The presentation of results will be material oriented so that the results of all tests on MX-80 will be presented in Section 3.2, on Deponit CaN in Section 3.3 and on ion exchanged MX-80 in Section 3.4.

3.2 MX-80

3.2.1 Basic data

Three types of MX-80 samples were tested. The first type was made by compaction of powder to a size that fitted the test equipment just before the test. The second type of specimen was trimmed from a larger block previously compacted at Clay Technology AB . The third type of specimen was trimmed from a sample initially taken from the same larger block as the second specimen but then also exposed to high water pressure according to Harrington and Birchall (2007). The three different types of specimen were labelled *lab compacted*, *block before water pressure* and *block after water pressure*, respectively.

The specimens representing the *block after water pressure* had been exposed to a stress and pressure history given by Harrington (2008, pers. comm.). According to this stress and pressure history a sample was taken from the larger block mentioned above and mounted in a device where the swelling pressure was determined to 5.1 MPa. The pore water pressure, starting from 1 MPa, was increased in steps to 37 MPa and then decreased in steps back to 1 MPa. After the exposure to the high pore water pressure the swelling pressure was determined to 8.4 MPa. The specimen was dismantled and further studied regarding swelling pressure and shear strength in the present investigation and called *block after water pressure*.

The initial water content, density, void ratio and degree of saturation determined for the three types of specimen are presented in Table 3-1. For the determination of void ratio and degree of saturation the particle density ρ_s = 2,780 kg/m^3 and water density ρ_w = 1,000 kg/m^3 were used. The values representing the lab compacted specimen are average values over the height of an extra specimen divided into three parts. The values representing the *block before water pressure* are average values of six determinations made at different positions of the block used and this is also the case for the seven determinations representing the *block after water pressure*.

In addition, some specimens were compacted from powder with lower initial water content, approximately 9%. These specimens were placed in a saturation device to be saturated before the coming tests.

Table 3-1. Average values of w, ρ, e and S_r.

	Lab compacted	Block before w.p.	Block after w.p.
w (%)	27.2	25.5	27.2
ρ (kg/m^3)	2,010	2,010	2,020
e	0.76	0.73	0.75
S_r (%)	99	97	100

3.2.2 Relative humidity

The resulting relative humidity measured above two specimens is shown in Table 3-2.

Table 3-2. Measured relative humidity and calculated corresponding suction.

	Block before w.p.	Block after w.p.
w (%)	26.2	27.2
e	0.73	0.75
RH (%)	91.9	93.0
T (˚C)	22.2	21.3
ψ_{calc} (kPa)	11,540	9,830

3.2.3 Swelling pressure

Figure 3-1 shows the swelling pressure measured on trimmed specimens that were allowed to swell a little from the *block before water pressure* and the *block after water pressure*. Table 3-3 shows the base variables and the evaluated swelling pressures.

Table 3-3. Result from swelling pressure tests. w, ρ, e and S_r are given both as initial and final values (initial/final).

	MX-80 Block before w.p. SP1	MX-80 Block after w.p. SP2
w (%)	26.1/30.6	27.0/31.1
ρ (kg/m^3)	2,020/1,970	2,010/1,960
e	0.74/0.84	0.75/0.86
S_r (%)	98/101	100/101
Swelling from initial state		
ΔH (mm)	0	0
ΔD (mm)	0.8	0.9
Swelling pressure		
P_s (kPa)	4,700	4,021

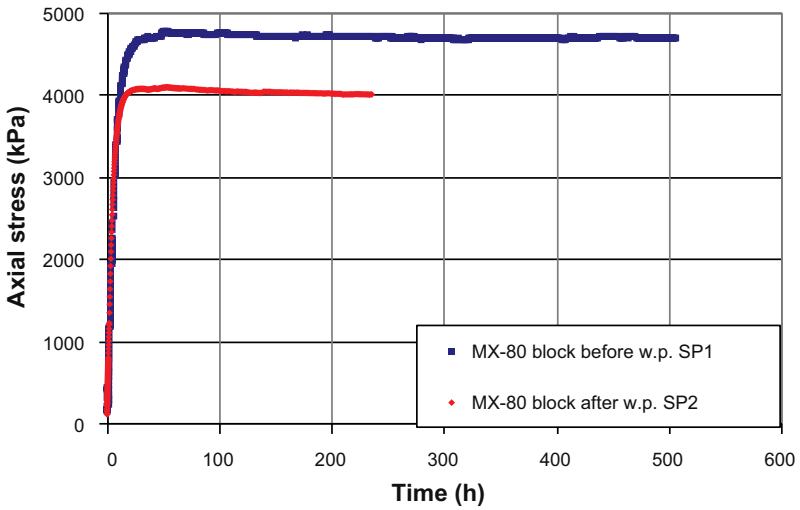

Figure 3-1. *Resulting swelling pressures from swelling pressure tests on specimens of MX-80 with densities of 1,960–1,970 kg/m^3.*

The samples were trimmed from a larger specimen and to be able to put it into the equipment the mechanically worked samples had a diameter slightly less than 35 mm. During the water uptake a radial swelling took place and the increase in dimensions is mentioned as "swelling from initial state" in Table 3-3. A consequence of the swelling was a lower final density and lower swelling pressure than originally.

3.2.4 Triaxial test

Triaxial tests were run on the three different types of specimen described above. Figure 3-2 shows the measured deviator stress vs. strain from the triaxial tests and Table 3-4 shows the base variables determined after the tests together with the evaluated mean stress and strain at maximum deviator stress. More results from each test can be found in Appendix 2.

Table 3-4. Results from the triaxial test series. w, ρ, e and S_r are given both as initial and final values (initial/final).

	MX-80 Lab compacted T1	**MX-80 Block before w.p. T2**	**MX-80 Block after w.p. T3**
w (%)	27.9/29.8	25.5/29.0	27.2/27.2
ρ (kg/m^3)	1,960/1,980	2,010/1,990	2,020/2,020
e	0.81/0.82	0.73/0.80	0.75/0.75
S_r (%)	96/101	97/101	100/101
At start of shearing			
σ_3 (kPa)	7,400	10,220	8,820
u (kPa)	850	1,170	730
p' (kPa)	6,550	9,050	8,090
Shearing rate (mm/s)	**$5\cdot10^{-6}$**	**$5\cdot10^{-6}$**	**$5\cdot10^{-6}$**
At maximum deviator stress			
q_{max} (kPa)	2,170	2,835	2,704
p'(kPa)	6,655	9,130	7,923
ε (%)	8	10.2	7.9

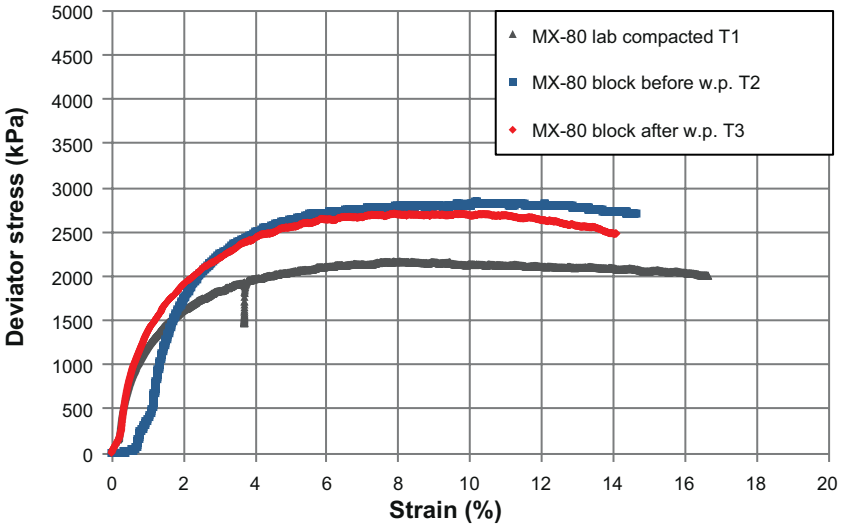

Figure 3-2. *Resulting deviator stress vs. strain from triaxial tests on three specimens of MX-80 with densities of 1,980–2,020 kg/m^3.*

3.2.5 Unconfined compression test

A series of unconfined compression tests was performed on the three types of specimen described above. Figure 3-3 shows the results. Doublet specimens were used, i.e. two *lab compacted* specimens compacted to the correct dimension, two samples trimmed from the *block before water pressure* and two samples trimmed from the *block after water pressure*. In Table 3-5 the base variables are presented with the evaluated maximum deviator stress and the corresponding strain. The height of the specimens was 40 mm and the rate of the shearing was 0.005 mm/s.

A series of unconfined compression tests was also made at an average temperature of 12˚C. In Appendix 6 the set-up used is briefly described and a temperature measurement made during a reference test is shown. The results from the tests are shown in Figure 3-4 and Table 3-6.

Finally, two series of unconfined compression tests were carried out at high rates at two different densities. Shearing rates between 0.003 mm/s and 300 mm/s were used in these series. The results are shown in Figures 3-5 and 3-6. The results are also shown in a table in Appendix 7.

Table 3-5. Results from the unconfined compression tests. w, ρ, e and S_r are given both as initial and final values (initial/final).

	MX-80 Lab compacted		**MX-80 Block before w.p.**		**MX-80 Block after w.p.**	
	UC1	UC2	UC3	UC4	UC5	UC6
w (%)	27.7/26.5	27.7/26.6	24.7/24.8	25.2/25.3	27.0/26.7	26.9/26.9
ρ (kg/m^3)	2,010/2,010	2,010/2,010	2,010/2,020	2,010/2,010	2,010/2,020	2,020/2,030
e	0.77/0.75	0.77/0.76	0.72/0.72	0.73/0.73	0.76/0.74	0.75/0.74
S_r (%)	100/98	100/98	95/96	96/96	99/100	100/101
At maximum deviator stress						
q_{max} (kPa)	2,580	2,400	3,250	3,150	2,860	2,850
ε (%)	6.5	7.4	5.5	5	5.5	6.2

Table 3-6. Results from unconfined compression tests at an average of 12˚C on MX-80.

	MX-80 12˚C UC1	**MX-80 12˚C UC3**
w (%)	28.8	25.8
ρ (kg/m^3)	1,980	2,020
e	0.80	0.74
S_r (%)	98	99
At maximum deviator stress		
q_{max} (kPa)	2,098	2,744
ε (%)	5.9	5.4

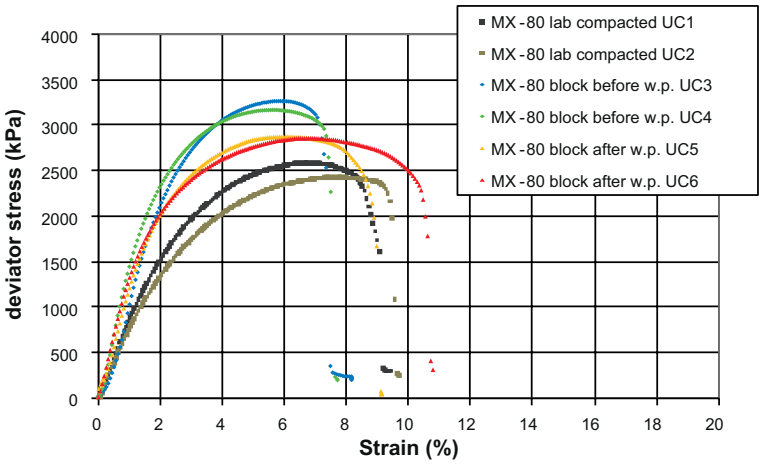

Figure 3-3. *Resulting deviator stress vs. strain from unconfined compression tests on specimens of MX-80 with densities of 2,010–2,030 kg/m³.*

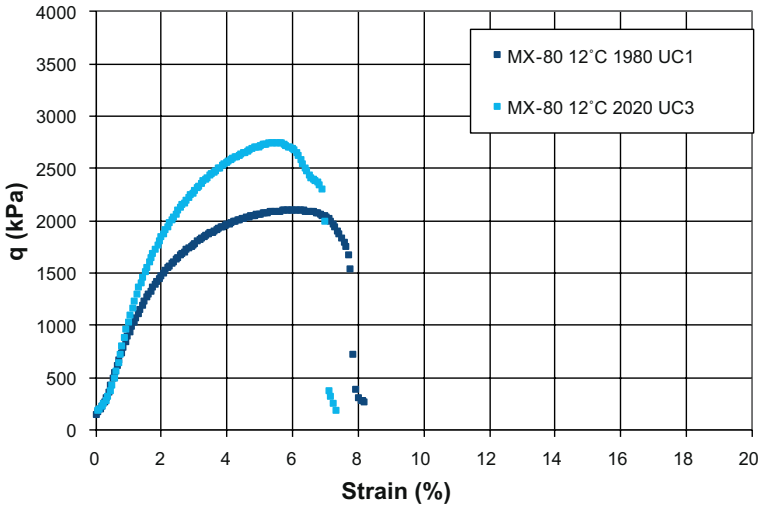

Figure 3-4. *Results from the unconfined compression test at an average temperature of 12˚C on MX-80 specimens. Densities (kg/m³) are shown in the legend.*

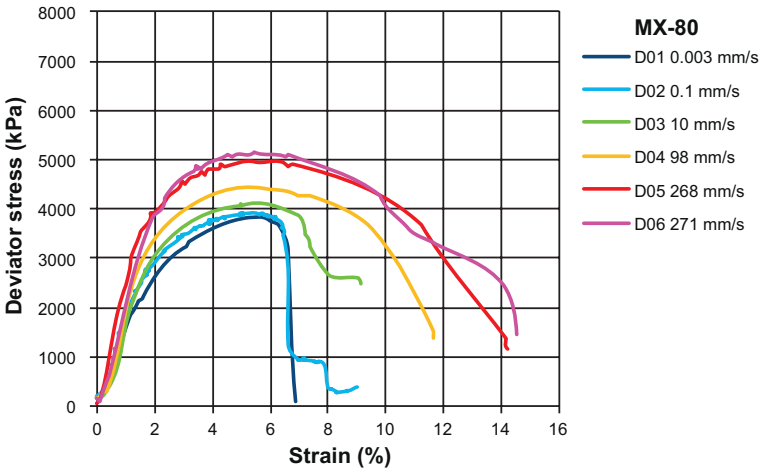

Figure 3-5. *Results from unconfined compression tests at high rates on MX-80 specimens with an average density of 2,040 kg/m³.*

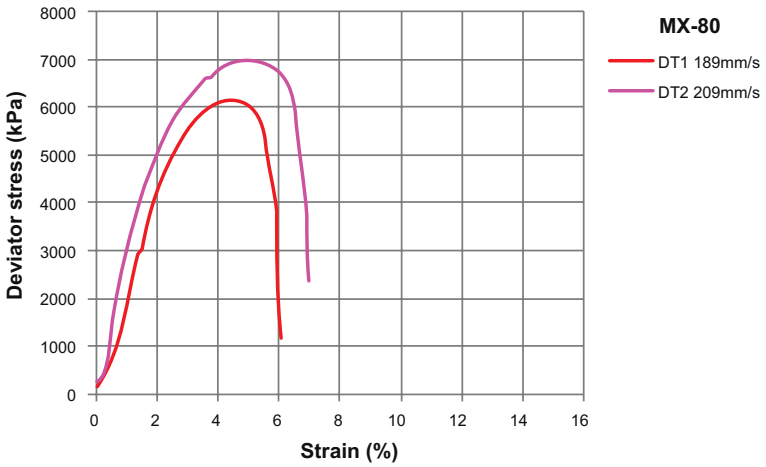

Figure 3-6. *Results from unconfined compression test at high rates on MX-80 specimens with an average density of 2,080 kg/m³.*

3.3 Deponit CaN

3.3.1 Basic data

The main part of the Deponit CaN specimens was compacted from powder with the initial water content 18.4% and then saturated in one of the saturation devices. The remaining part of the specimens was compacted from powder with the initial water content 23% to almost full saturation. For the determination of void ratio and degree of saturation the particle density ρ_s = 2,750 kg/m³ and water density ρ_w = 1,000 kg/m³ have been used.

3.3.2 Swelling pressure

The swelling pressure was determined on one specimen according to the technique described in Section 2-5, DepCaN_SP1. However, measurement with a slightly different technique was carried out during saturation of specimens intended for the triaxial tests. Figure 3-7 and Table 3-7 show the results from the swelling pressure measurements. Pore water pressure was applied during some of the tests. This was decreased to zero at least 1 day before dismantling.

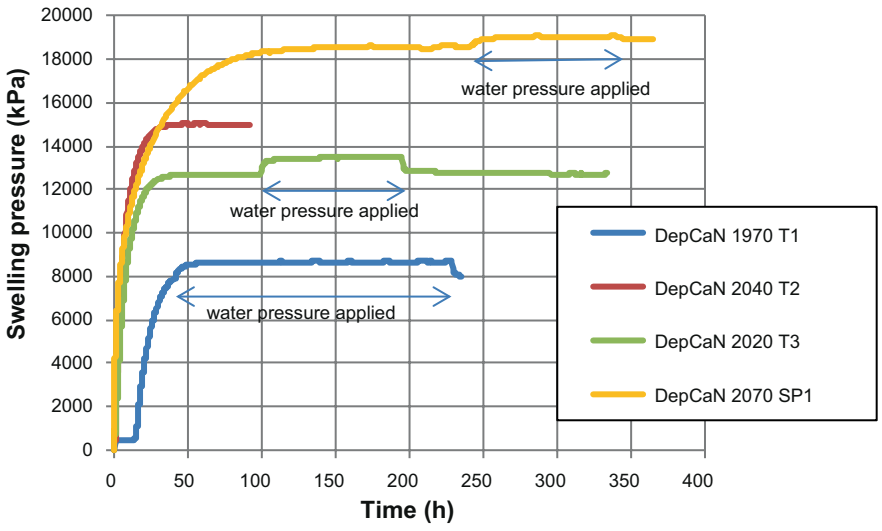

Figure 3-7. *Measured swelling pressure during saturation of the Deponit CaN specimens. Pore water pressure was applied during some of the testing time of some of the specimens. Densities (kg/m³) are shown in the legends.*

Table 3-7. Result from measurement of swelling pressure during saturation.

	DepCaN T1	DepCaN T2	DepCaN T3	DepCaN SP1
w (%)	27.6	24.0	25.9	23.0
ρ (kg/m^3)	1,970	2,040	2,020	2,070
e	0.78	0.67	0.71	0.63
S_r (%)	97	98	100	100
Swelling during dismantling				
ΔV/V (%)	2	1.5	1.2	not measured
Swelling pressure				
P_s (kPa)	8,030	14,990	12,710	18,930

Of the three specimens intended for triaxial testing only two were used for that purpose; DepCaN_1 and DepCaN_3. The specimen DepCaN_2 was instead cut to pieces and the water content and density determined according to standard testing. The two specimens used for triaxial testing could not be cut to pieces until after the triaxial tests. Instead the water contents were estimated from the change in mass from the initial water content and the densities were estimated from a volume determined by a slide calliper, which both deviate from the ordinary ways of determination of water content and density.

3.3.3 Triaxial test

The measured deviator stress vs. strain from the triaxial tests is presented in Figure 3-8. In Table 3-8 the base variables determined after the test are presented together with the evaluated mean stress and strain at maximum deviator stress. More results from each test can be found in Appendix 2.

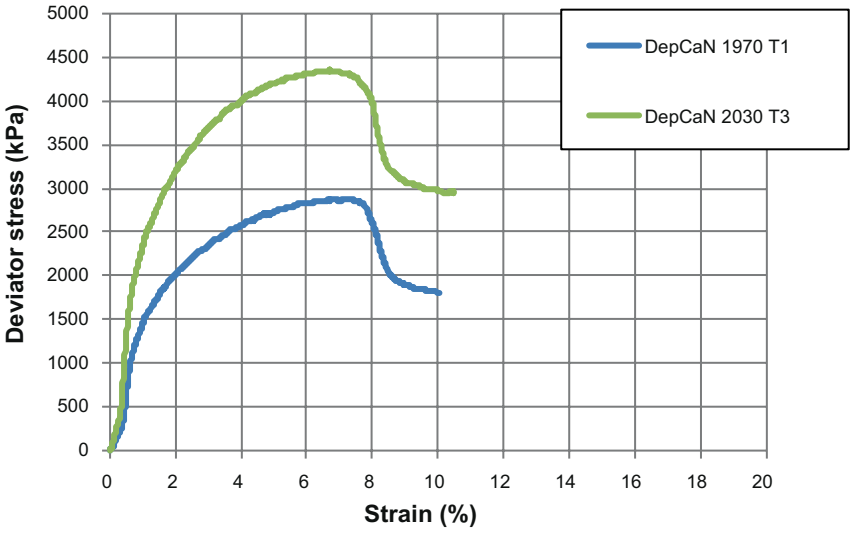

Figure 3-8. *Resulting deviator stress vs. strain from triaxial tests on two specimens of Deponit CaN. Densities (kg/m^3) are shown in the legends.*

Table 3-8. Results from the triaxial test series. w, ρ, e and S_r are given both as initial and final values (initial/final). (1- the final values are determined as average over the specimens without end pieces.)

	DepCaN T1	DepCaN T3
w (%)	27.6/29.6[1]	25.9/25.8[1]
ρ (kg/m^3)	1,970/1,970[1]	2,020/2,030[1]
e	0.78/0.81[1]	0.71/0.70[1]
S_r (%)	97/100[1]	100/100[1]
At start of shearing		
σ_3 (kPa)	8,743	12,875
u (kPa)	788	1,335
p' (kPa)	7,955	11,540
Shearing rate (mm/s)	**$4.25 \cdot 10^{-6}$**	**$4.5 \cdot 10^{-6}$**
At maximum deviator stress		
q_{max} (kPa)	2,879	4,349
p'(kPa)	7,815	12,256
ε (%)	7.3	6.7

3.3.4 Unconfined compression test

In one series of unconfined compression tests under ordinary conditions three Deponit CaN specimens were tested. The results are shown in Figure 3-9 and Table 3-9.

Table 3-9. Results from one series of unconfined compression tests on Deponit CaN.

	DepCaN UC11	DepCaN UC13	DepCaN UC15
w (%)	31.0	28.5	24.8
ρ (kg/m^3)	1,970	2,000	2,050
e	0.84	0.77	0.67
S_r (%)	102	102	101
At maximum deviator stress			
q_{max} (kPa)	2,260	3,340	5,250
ε (%)	6.0	7.2	5.1

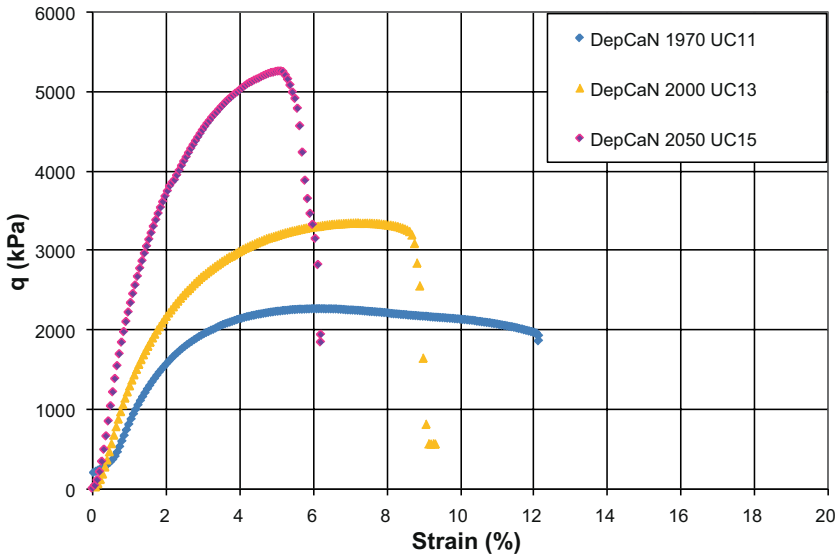

Figure 3-9. *Results from one series of unconfined compression tests on Deponit CaN. Densities (kg/m^3) are shown in the legends.*

A series of unconfined compression tests was also carried out at an average temperature of 12˚C. In Appendix 6 the set-up used is briefly described and a temperature measurement made during a reference test is shown. The results from the tests are shown in Figure 3-10 and Table 3-10. One of the specimens UC5 slipped and was re-mounted twice before the test could be accomplished. The problem was probably due to slightly tilting end surfaces.

Finally, two series of unconfined compression tests were performed at higher rates at two different densities. Shearing rates between 0.003 mm/s and 300 mm/s were used in these series. The results are shown in Figures 3-11 and 3-12. The results are also shown in a table in Appendix 7.

Table 3-10. Results from unconfined compression tests at lower temperature on DepCaN.

	DepCaN 12˚C UC5	DepCaN 12˚C UC7	DepCaN 12˚C UC9
w (%)	31.7	28.2	25.0
ρ (kg/m^3)	1,960[1]	1,990	2,040
e	0.85	0.77	0.69
S_r (%)	102	101	101
At maximum deviator stress			
q_{max} (kPa)	2,185	2,931	4,863
ε (%)	4.8	7.2	6.9

[1] Specimen re-mounted twice due to slipping.

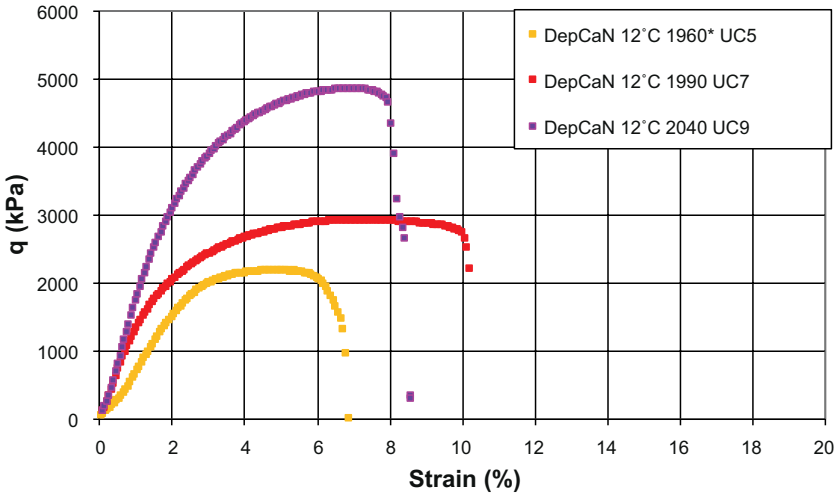

Figure 3-10. *Results from unconfined compression test at lower temperature on Deponit CaN. Densities (kg/m^3) are shown in the legends.*

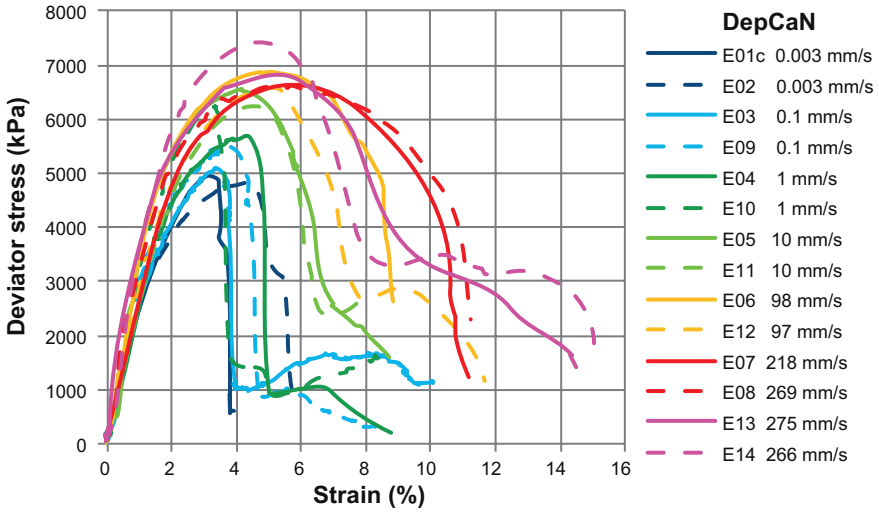

Figure 3-11. *Results from shearing at high rates on specimens of DeponitCaN with a density of 2,050 kg/m³.*

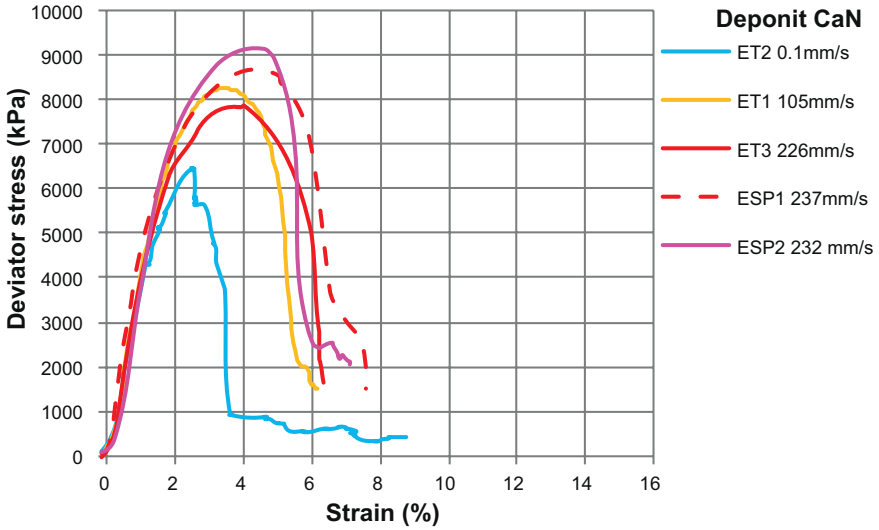

Figure 3-12. *Results from shearing at high rates on specimens of DeponitCaN with a density of 2,070 kg/m³.*

3.4 Ion exchanged MX-80

3.4.1 Basic data

Two types of ion exchanged clays were prepared from MX-80; one sodium bentonite MX-80Na and one calcium bentonite MX-80Ca. Specimens of MX-80 were compacted and placed in devices for saturation. After water saturation the ion exchange was made by changing the circulating solution around the specimens. The process of ion exchange is described in Appendix 1.

Compacted MX-80 powder with the initial water content of 9% was used for the ion exchanged specimens. For the determination of void ratio and degree of saturation the particle density ρ_s = 2,780 kg/m³ and water density ρ_w = 1,000 kg/m³ were used.

3.4.2 Relative humidity

The relative humidity was measured above pieces from the specimens used for the measurement of swelling pressure, presented below. The results are shown in Table 3-11.

Table 3-11. Measured relative humidity and calculated corresponding suction for ion exchanged materials.

	MX-80Ca_SP1	MX-80Ca_SP2	MX-80Ca_SP3	MX-80Ca_SP4
w (%)	30.0	28.9	22.6	23.1
e	0.84	0.81	0.65[1] (0.63)	0.7[1] (0.64)
RH (%)	94.4	94.5	87.0	89.2
T (˚C)	20.6	20.5	20.4	20.5
ψ_{calc} (kPa)	7,812	7,652	18,953	15,489

[1] Specimens having low degrees of saturation. Values in brackets are calculated from the measured water contents and an assumption of full saturation (S_r = 100%).

3.4.3 Swelling pressure

The swelling pressure of MX-80Ca was measured. The measurements were done during the ion exchanged process, from MX-80 to MX-80Ca. Figure 3-13 and Table 3-12 show the results.

From the specimens SP3 and SP4 the resulting degree of saturation was low, 96% and 92% respectively. These values were based on densities determined in the ordinary way which includes submerging the specimens into paraffin oil. The densities were also calculated in a second way, from the measured water contents and an assumption of full saturation (S_r = 100%). For the actual tests the calculated values, based on this second way of determining density, are shown in brackets in Table 3-12.

Finally, the densities were also estimated from the volume inside the equipment and the in this way estimated densities were similar to the densities determined with the second method. Thus, large swelling did occur during dismantling of SP4, 5%, and the results presented in Figures 4-1 to 4-3 are plotted versus both the measured and the calculated void ratio for this specimen.

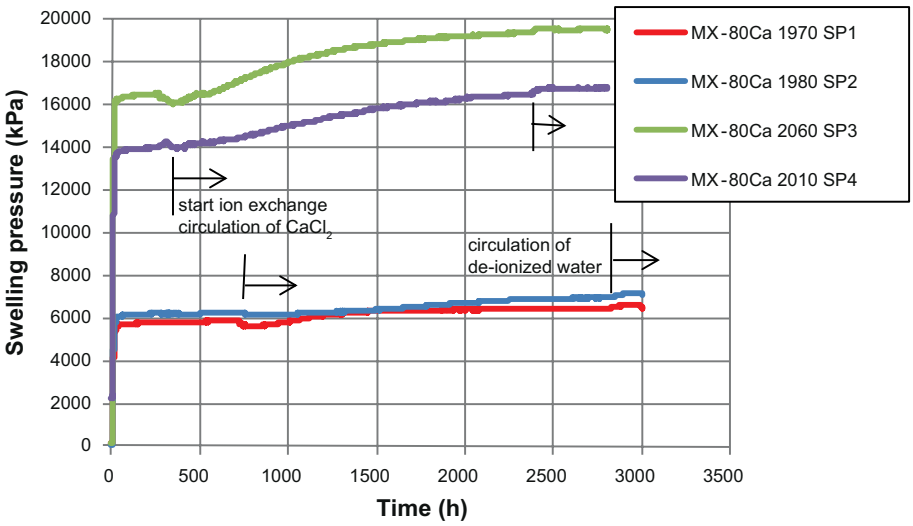

Figure 3-13. *Swelling pressure of MX-80Ca measured during the ion exchange. Densities (kg/m³) are shown in the legends.*

Table 3-12. Result from measurement of swelling pressure of MX-80Ca during ion exchange.

	MX-80Ca SP1	MX-80Ca SP2	MX-80Ca SP3[1]	MX-80Ca SP4[1]
w (%)	30.0	28.9	22.6	23.1
ρ (kg/m^3)	1,970	1,980	2,060 (2,090)	2,010 (2,080)
e	0.84	0.81	0.65 (0.63)	0.70 (0.64)
S_r (%)	100	99	96 (100)	92 (100)
Swelling during dismantling				
$\Delta V/V$ (%)	< 0.1	< 0.1	0.4	5
Swelling pressure				
P_s (kPa) MX-80	5,820	6,150	16,360	13,900
P_s (kPa) MX-80Ca	6,570	7,090	19,520	16,750

[1] Specimens having low degrees of saturation. Values in brackets are calculated from the measured water contents and an assumption of full saturation (S_r = 100%).

3.4.4 Triaxial test

Ion exchange was made on compacted MX-80 specimens having a height of 10 mm. For each triaxial test seven such specimens were needed to get the final height of 70 mm. Since eight 10 mm specimens were ion-exchanged in each series the last one was used for the determination of *RH*. Measured *RH* is shown in Table 3-13.

For two specimens MX-80Ca T2 and MX-80Na T1 the chloride solutions used during the ion exchange were kept and also used as pore water in the drainage system during the triaxial tests. The chloride solutions used were 0.3M $CaCl_2$ and 0.6M NaCl corresponding to a salt content of approximately 4.2 weight% and 3.5 weight%, respectively. For these specimens the chloride solutions were used as reference in the calculation of corresponding suction according to Section 2.4 with the vapour pressure p_e calculated from *RH* measurements which gave 98.3% and 97.7% for 0.3M $CaCl_2$ and 0.6M NaCl, respectively.

Figure 3-14 shows the measured deviator stress vs. strain in the triaxial tests. Table 3-14 shows the base variables determined after the test and the evaluated mean stress and strain at maximum deviator stress. More results from each test can be found in Appendix 2.

The influence of shear rate on the deviator stress was studied after finished shearing of the specimen MX-80Ca T1, still inside the triaxial cell. The rate was increased 10, 100 and 1,000 times. The results are shown in Appendix 5. An attempt to correct the stresses to the rate was done and this is further commented on in Section 4.3.

Table 3-13. Measured relative humidity and calculated suction for the ion exchanged materials.

	MX-80Ca T1	MX-80Ca T2	MX-80Ca T3	MX-80Na T1
w (%)	29.3	29.2	25.7	30.3
e	0.82	0.81	0.72	0.86
RH (%)	95.1	93.9	90.8	94.6
T (˚C)	20.1	20.9	21.3	20.0
ψ_{calc} (kPa)	6,740	6,320[1] (8,620)	13,140	4,460[1] (7,560)

[1] The value was calculated with the chloride solution used as reference.

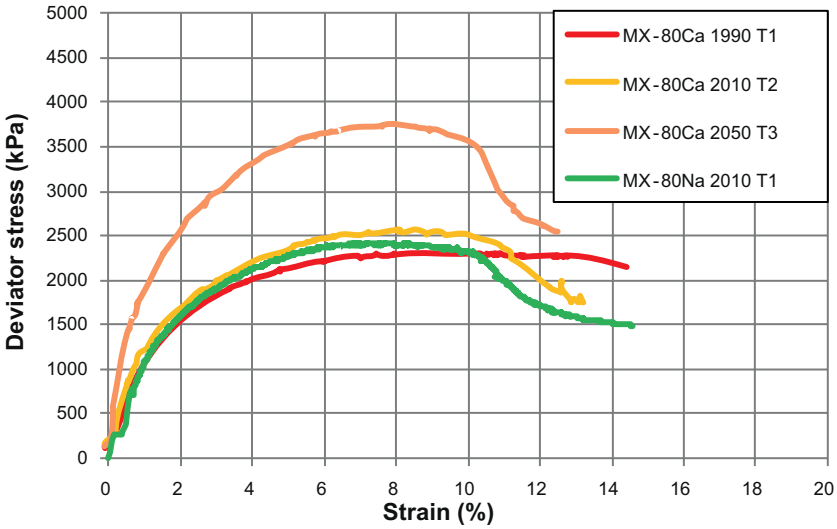

Figure 3-14. *Resulting deviator stress vs. strain from triaxial tests on ion exchanged material MX-80Ca and MX-80Na. Densities (kg/m³) are shown in the legends.*

Table 3-14. Results from the triaxial test series. w, ρ, e and S_r are given both as initial and final values (initial/final). (1- the final values are determined as average over the specimens without end pieces.)

	MX-80Ca T1	MX-80Ca T2	MX-80Ca T3	MX-80Na T1
w (%)	29.3/29.1[1]	29.2/26.4[1]	25.7/24.3[1]	30.3/28.1[1]
ρ (kg/m³)	1,970/1,990[1]	1,980/2,010[1]	2,030/2,050[1]	1,940/2,010[1]
e	0.82/0.81[1]	0.81/0.75[1]	0.72/0.69[1]	0.86/0.77[1]
S_r (%)	99/100[1]	100/99[1]	99/98[1]	97/101[1]
At start of shearing				
σ_3 (kPa)	7,410	8,030	12,110	8,441
u (kPa)	990	590	1,010	960
p' (kPa)	6,420	7,440	11,100	7,480
Shearing rate (mm/s)	$9.1 \cdot 10^{-6}$	$4.7 \cdot 10^{-6}$	$5.2 \cdot 10^{-6}$	$4.4 \cdot 10^{-6}$
Water	De-ionized	0.3M $CaCl_2$	De-ionized	0.6M NaCl
At maximum deviator stress				
q_{max} (kPa)	2,310	2,580	3,740	2,410
p'(kPa)	6,470	7,940	12,370	7,800
ε (%)	9.4	8.6	7.7	7.2

3.4.5 Unconfined compression test

Unconfined compression tests were performed on the purified WyNa and WyCa. These purified materials were ion exchanged from MX-80 according to Karnland et al. (2006) and all accessory minerals were removed. The tests in the present investigation were done to study the difference between the sodium,WyNa, and the calcium,WyCa, bentonite. This test series was the only one using specimens with the height equal to the diameter, i.e. 20 mm. This could be done since determination of strength was not the purpose of the test series. The rate of the shearing was 0.003 mm/s. The results are shown in Figure 3-15 and Table 3-15.

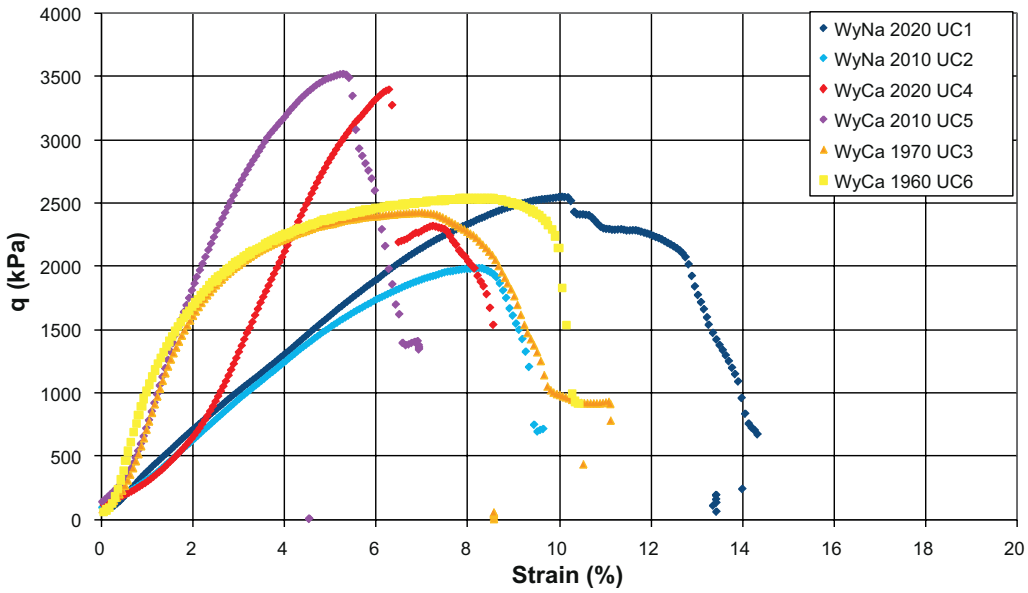

Figure 3-15. *Resulting deviator stress vs. strain from unconfined compression tests on ion exchanged purified materials. Densities (kg/m³) are shown in the legends.*

Table 3-15. Results from the unconfined compression test series. w, ρ, e and S_r are given as final values.

	WyNa UC1	WyNa UC2	WyCa UC3	WyCa UC4	WyCa UC5	WyCa UC6
w (%)	26.8	28.16	31.3	27.1	27.5	30.9
ρ (kg/m³)	2,020	2,010	1,970	2,020	2,010	1,960
e	0.74	0.78	0.86	0.75	0.76	0.86
S_r (%)	100	101	101	100	101	100
At maximum deviator stress						
q_{max} (kPa)	2,540	1,990	2,422	3,400	3,520	2,540
ε (%)	10.0	8.2	6.8	6.3	5.3	8.4

4 Compilation and analysis of test results

4.1 General

In this chapter the laboratory test results from this investigation are summarized. Additional analyses and evaluations are done by Börgesson et al. (2010).

4.2 Swelling pressure

The swelling pressure can be modelled as function of the void ratio according Equation 4-1 when $0.5 < e < 1.5$ according to Börgesson et al. (1995).

$$p = p_0 \cdot \left(\frac{e}{e_0} \right)^{(1/\beta)} \tag{4-1}$$

where

p swelling pressure (at e) (kPa)

e void ratio

e_0 reference void ratio see Table 4-1

p_0 reference swelling pressure (at e_0) see Table 4-1

β constant see Table 4-1

Measured swelling pressures of MX-80 are presented in Figure 4-1 together with Equation 4-1. The mean stress p' measured during the triaxial tests are included in the graph as a measure of the swelling pressure. *RH* measurements or calculated suction values are also used as a measure of the swelling pressure, Section 2.4. Results from ion exchanged MX-80Na are also shown.

In Figure 4-1 two specimens are put in brackets. One is the yellow diamond representing a specimen with a certain low degree of saturation from the determination of swelling pressure in Section 3.4, specimen *MX-80Ca SP4*. A lower void ratio was calculated from the measured water content and assuming full saturations see Table 3-12. This lower value of void ratio is also used in Figure 4-1.

The second specimen put in brackets is the specimen *MX-80 T2 block before w.p.* from Section 3.2. There is a question mark regarding the void ratio determined after the triaxial test and the result (blue solid circle) is put in brackets. The measured swelling pressure from this test is instead plotted with the void ratio from the start of the test, i.e. the point has been moved to the left and the brackets have been removed.

The question mark regarding this specimen comes from the dismantling of the specimen, MX-80 *T2*, when a thin layer with lower density was observed. This thin layer was intact when the water contents and densities were determined. However, in this case it is probable that the layer was an effect of the dismantling procedure and the determined water content thus too high. According to the analysis presented in Appendix 3 an outer layer with a thickness of 2.5 mm with a water content of 35% and a void ratio of 1 is needed to correspond to the measured average values of *w* and *e*.

Table 4-1. Constants used in Equation 4-1 valid for different materials.

Material	e_0	p_0 (kPa)	β	Reference
MX-80	1.1	1,000	–0.19	Börgesson et al. (1995)
Deponit CaN	1.33	1,000	–0.254	This investigation

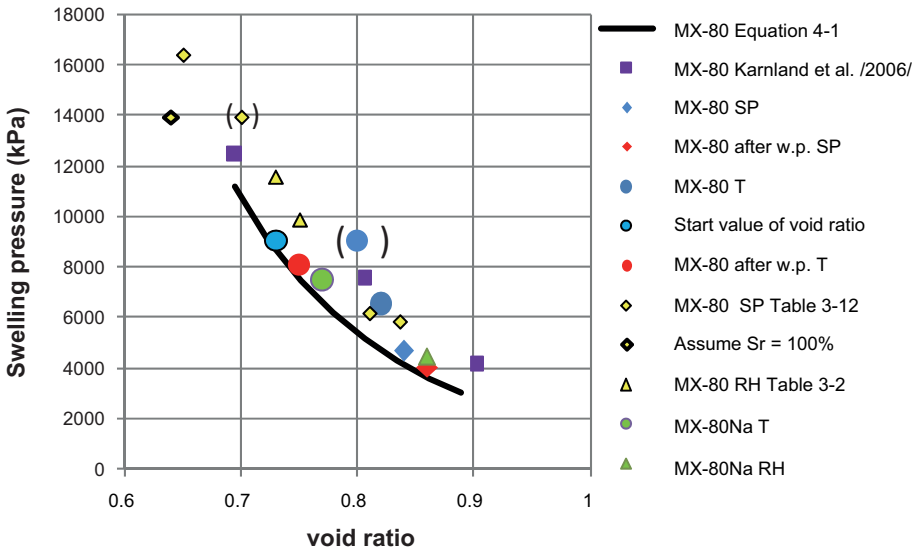

Figure 4-1. *Measurements of swelling pressure of MX-80 and ion exchanged MX-80Na done in this investigation; triaxial tests (circles), swelling pressure measurements (diamonds) and RH measurements (triangles). Measurements on the block before water pressure are blue and on block after water pressure red. Results from Karnland et al. (2006) are also shown. Specimens put in brackets have been moved to the left.*

In Figure 4-2 the results from Figure 4-1 are presented together with measurements done before and after application of high water pressure by Harrington and Birchall (2007), MX80-11 BGS, and Harrington (2008, pers. comm.), MX80-12 BGS. Figure 4-2 also shows two retention curves representing wetting and drying (Dueck and Nilsson 2010). Void ratios have been calculated from the water contents of the retention curves and the assumption of full saturation. The two retention curves seem to form a boundary for possible stresses where the difference then could be caused by hysteresis and anisotropy.

Swelling pressures determined on Deponit CaN and ion exchanged MX-80Ca are presented in Figure 4-3. Results from triaxial tests and *RH* measurements are also shown. A line fitted to Equation 4-1 with the parameters shown in Table 4-1 is included in the diagram. The results put in brackets represent the same specimen as the yellow diamond in Figure 4-1 and Figure 4-2 but after the ion exchange. In Figure 4-3 both swelling pressure and *RH* were determined on this specimen. The results are accordingly corrected.

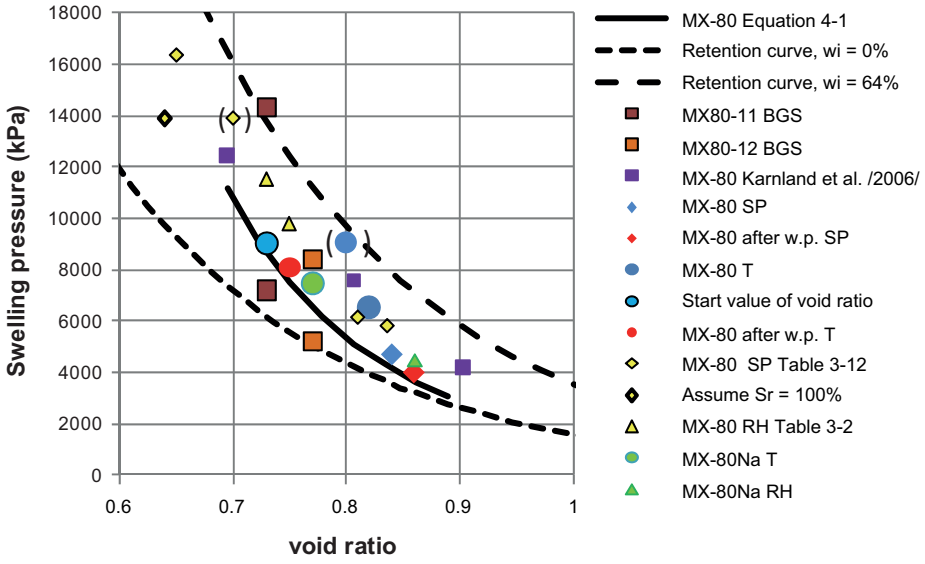

Figure 4-2. *Figure 4-1 together with retention curves presented by Dueck and Nilsson (2010). Swelling pressures from Harrington and Birchall (2007) (MX80-11 BGS) and Harrington (2008, pers. comm.) (MX80-12 BGS) before and after application of high water pressure are also shown.*

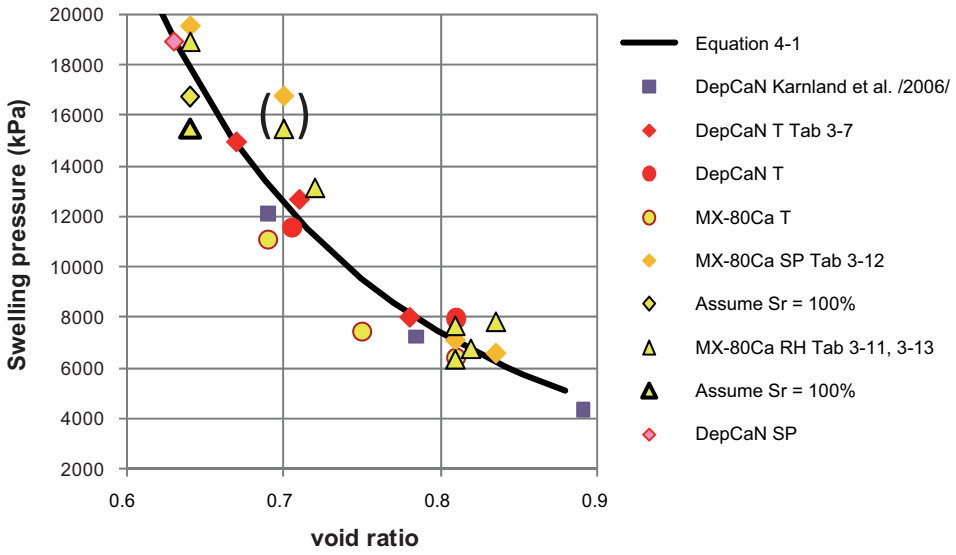

Figure 4-3. *Measurements of swelling pressure of Deponit CaN and ion exchanged MX-80Ca done in this investigation; triaxial tests (circles), swelling pressure measurements (diamonds) and RH measurements (triangles). Results from Karnland et al. (2006) are also shown. Specimens put in brackets have been moved to the left.*

4.3 Shear strength

The measured shear strength, i.e. maximum deviator stress, can be compared to results from the literature. The failure envelope, i.e. the shear strength plotted as function of the mean stress has been proposed to be expressed according to Equation 4-2 (Börgesson et al. 1995), which originally was derived from triaxial test results.

$$q_f = q_{f0} \cdot \left(\frac{p}{p_0} \right)^b \qquad (4\text{-}2)$$

where

q_f deviator stress at failure at swelling pressure p (kPa)

q_{f0} deviator stress at failure at the swelling pressure p_0 see Table 4-2

b constant see Table 4-2

Figure 4-4 shows the results from this investigation together with results from other investigations. Figure 4-4 is plotted in Appendix 4 with the stress paths included for all tests conducted in this investigation.

The failure envelopes of the bentonite materials have been evaluated according to Equation 4-2. The resulting parameters are shown in Table 4-2 and the curves are plotted in Figure 4-4.

Table 4-2. Constants used in Equation 4-2 valid for different materials.

Material	b	q_{f0} (kPa)	Reference
Na-bentonite MX-80	0.77	500	Börgesson et al. (1995)
Ca-benonite Moosburg	0.77	750	Börgesson et al. (1995)
Ion exchanged MX-80Ca	0.77	540	This investigation
Deponit CaN	0.77	610	This investigation

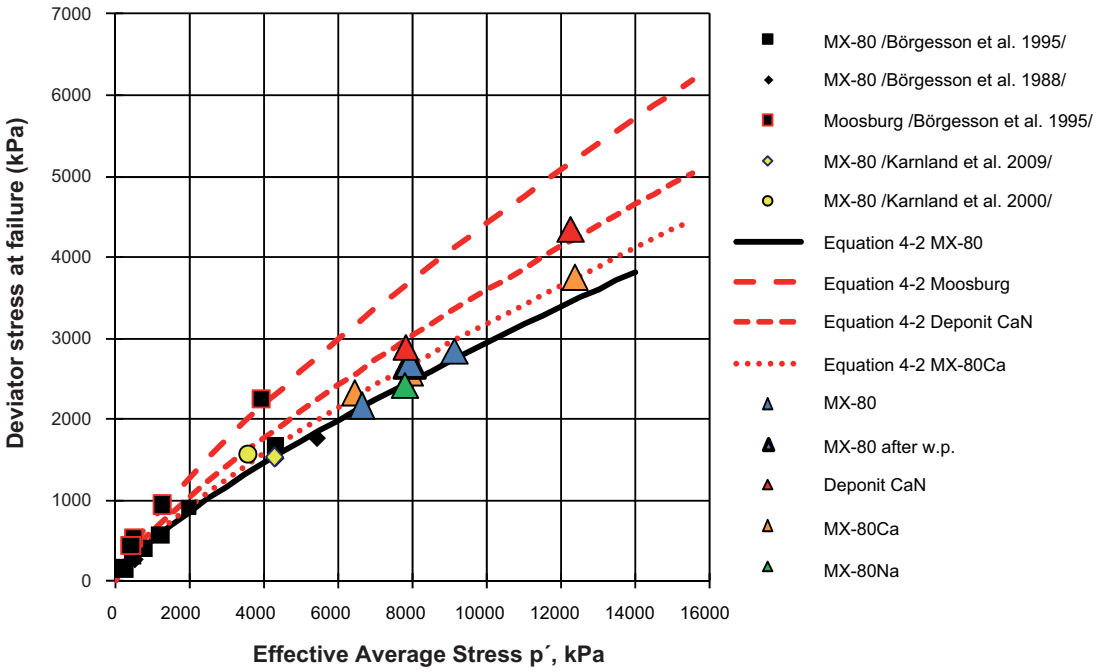

Figure 4-4. *Results from triaxial test series compared to test results from Karnland et al. (2000, 2009) (yellow) and Börgesson et al. (1988, 1995) (black).*

The triaxial test made on MX-80 T3 after exposure to a high water pressure shows a slightly higher strength compared to other tests on MX-80. However, the difference is small and is considered to be within the margin of natural scatter so the conclusion is that the history of high water pressure did not yield an increase in shear strength. Unconfined compression tests made on the same materials confirm these results.

Deviator stress versus void ratio resulting from the unconfined compression tests are plotted together with results from the triaxial tests in Figure 4-5. In this figure the lines represent a combination of Equation 4-1 and 4-2 to get the relation between deviator stress q and void ratio e.

In addition to the maximum deviator stress the corresponding strain, shown in Chapter 3, can be used for the stress-strain relation. This is further analysed by Börgesson et al. (2010).

Finally, the dependence of shear rate on shear strength has been proposed to follow Equation 4-3 (Börgesson et al. 2004).

$$q_{fs} = q_{fs0} \cdot \left(\frac{v_s}{v_{s0}} \right)^n \qquad (4\text{-}3)$$

where

v_s shear rate (m/s)

v_{s0} reference shear rate

q_{fs} deviator stress at failure at shear rate v_s

q_{fs0} deviator stress at failure at the reference shear rate

n factor describing the rate dependence

The influence of shear rate on the deviator stress was studied after finished shearing in one of the triaxial tests, with the specimen still inside the triaxial cell. An attempt to correct the stresses to the rate used was done by use of Equation 4-3. The result, shown in Appendix 5, indicates that if the constant n equals 0.065, as suggested for MX-80 by Börgesson et al. (2004), the influence of deformation rate seems to be too strong for rates from $1{\cdot}10^{-8}$ to $1{\cdot}10^{-5}$ m/s.

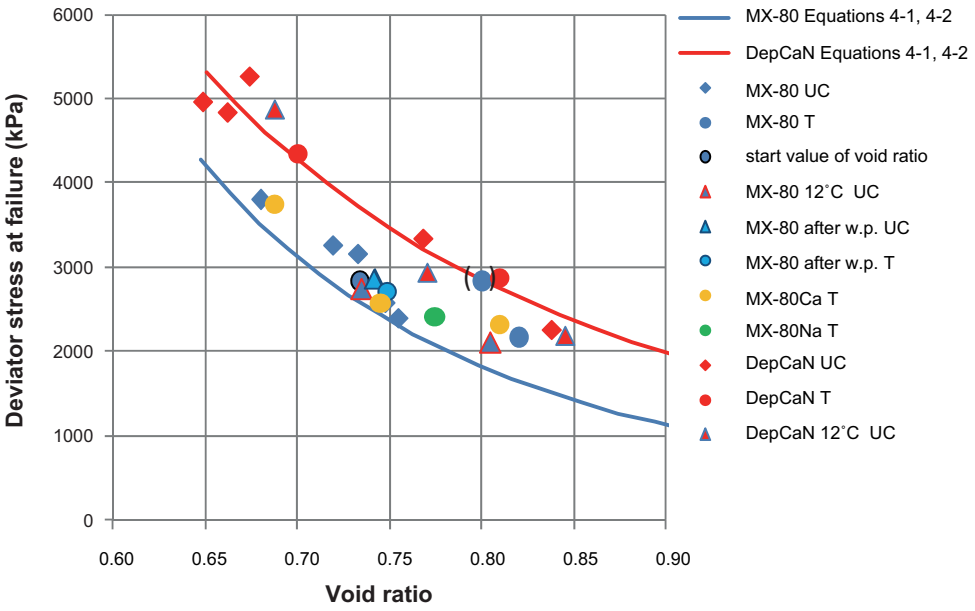

Figure 4-5. *Results from unconfined compression tests (UC) and triaxial tests (T) on MX-80 (blue), MX-80Na (green), MX-80Ca (orange) and DepCaN (red).*

Figure 4-6 shows deviator stress at failure vs. strain rate. The lines represent Equation 4-3 and the open symbols are data from Börgesson et al. (2004) and Karnland et al. (2000, 2009). Observe that the strain rate (%/s) is plotted instead of shear rate (mm/s). The reason for this change is that strain rate is more relevant both as phenomenological and modelling reasons. Results from this investigation are presented as filled symbols. The densities (kg/m^3) of these specimens are shown for tests run at low rates. All triaxial tests were run at rates lower than 0.0001%/s and test results at higher rates were obtained by unconfined compression tests.

The relation for Deponit CaN at the density 2,050 kg/m^3 is evaluated and plotted as a straight line in the diagram, which yields the parameter n = 0.038 in Equation 4-3 with shear rate exchanged for strain rate. For Equation 4-3 the deviator stress at failure at the reference shear rate q_{fs0} and the reference shear rate v_{s0} used are 8,000 kPa and 400 mm/s, respectively.

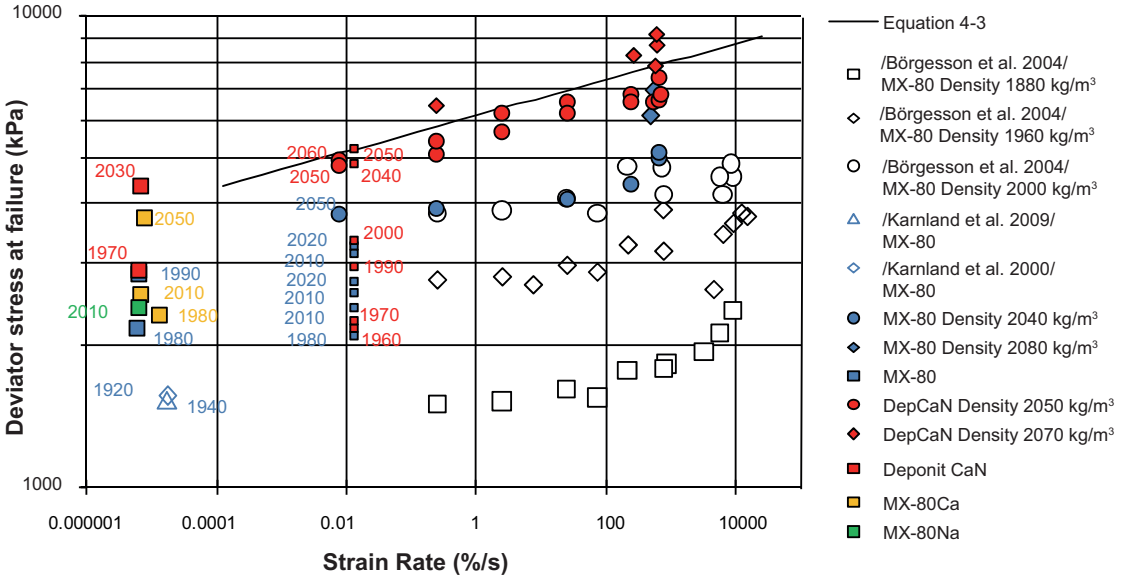

Figure 4-6. *Results from the triaxial and unconfined compression test series plotted together with data from Börgesson et al. (2004) and from Karnland et al. (2000, 2009). All triaxial tests were run at rates lower than 0.0001%/s and test results at higher rates were obtained by unconfined compression tests.*

5 Final comments

The test results from a laboratory study focused on undrained stress-strain-strength properties have been presented. The results are presented to be used as a basis for the reference material model presented by Börgesson et al. (2010).

6 References

SKB's (Svensk Kärnbränslehantering AB) publications can be found at www.skb.se/publications.

Börgesson L, Hernelind J, 2006. Earthquake induced rock shear through a deposition hole. Influence of shear plane inclination and location as well as buffer properties on the damage caused to the canister. SKB TR-06-43, Svensk Kärnbränslehantering AB.

Börgesson L, Hökmark H, Karnland O, 1988. Rheological properties of sodium smectite clay. SKB TR 88-30, Svensk Kärnbränslehantering AB.

Börgesson L, Johannesson L-E, Sandén T, Hernelind J, 1995. Modelling of the physical behaviour of water saturated clay barriers. Laboratory tests, material models and finite element application. SKB TR 95-20, Svensk Kärnbränslehantering AB.

Börgesson L, Johannesson L-E, Hernelind J, 2004. Earthquake induced rock shear through a deposition hole. Effect on the canister and the buffer. SKB TR-04-02, Svensk Kärnbränslehantering AB.

Börgesson L, Dueck A, Johannesson L-E, 2010. Material model for shear of the buffer. Evaluation of laboratory test results. SKB TR-10-31, Svensk Kärnbränslehantering AB.

Dueck A, Börgesson L, 2007. Model suggested for an important part of the hydro-mechanical behaviour of a water unsaturated bentonite. Engineering Geology, 92, pp 160–169.

Dueck A, Nilsson U, 2010. Thermo-Hydro-Mechanical properties of MX-80. Results from advanced laboratory tests. SKB TR-10-55, Svensk Kärnbränslehantering AB.

Fredlund D G, Rahardjo H, 1993. Soil mechanics for unsaturated soils. New York: Wiley.

Harrington J F, Birchall D J, 2007. Sensitivity of total stress to changes in externally applied water pressure in KBS-3 buffer bentonite. SKB TR-06-38, Svensk Kärnbränslehantering AB.

Hernelind J, 2010. Modelling and analysis of canister and buffer for earthquake induced rock shear and glacial load. SKB TR-10-34, Svensk Kärnbränslehantering AB.

Kahr G, Kraehenbuehl F, Stoeckli H F, Müller-Vonmoos M, 1990. Study of the water-bentonite system by vapour adsorption, immersion calorimetry and X-ray techniques: II. Heats of immersion, swelling pressures and thermodynamic properties. Clay Minerals, 25, pp 499–506.

Karnland O, Sandén T, Johannesson L-E, Eriksen T E, Jansson M, Wold S, Pedersen K, Motamedi M, Rosborg B, 2000. Long term test of buffer material. Final report on the pilot parcels. SKB TR-00-22, Svensk Kärnbränslehantering AB.

Karnland O, Muurinen A, Karlsson F, 2005. Bentonite swelling pressure in NaCl solutions – experimentally determined data and model calculations. In: Alonso E, Ledesma A (eds). Advances in understanding engineered clay barriers: proceedings of the International Symposium on Large Scale Field Tests in Granite, Sitges, Barcelona, 12–14 November 2003. London: Taylor & Francis Group, pp 241–256.

Karnland O, Olsson S, Nilsson U, 2006. Mineralogy and sealing properties of various bentonites and smectite-rich clay minerals. SKB TR-06-30, Svensk Kärnbränslehantering AB.

Karnland O, Olsson S, Dueck A, Birgersson M, Nilsson U, Hernan-Håkansson T, Pedersen K, Nilsson S, Eriksen T E, Rosborg B, 2009. Long term test of buffer material at the Äspö Hard Rock Laboratory, LOT project. Final report on the A2 test parcel. SKB TR-09-29, Svensk Kärnbränslehantering AB.

Appendix 1

Ion exchange of MX-80

General

The ion exchange was in general done by the following steps:

1. Specimens of MX-80 were compacted to eight cylindrical specimens with a height of 10 mm and a diameter of 35 mm.
2. The specimens were put in two saturation devices, four specimens in each device, with filters on both sides.
3. The specimens were saturated at constant volume condition by evacuating the air and maintained supply of de-ionized water.
4. After a couple of days the de-ionized water was changed to a chloride solution circulated through the filters above and below the specimens. The cation of the chloride solution was the same as the desired dominating cation of the clay (i.e. Na^+ or Ca^{2+}).
5. To keep a constant gradient the chloride solution was changed regularly. The concentration of the exchanged ion was measured with an ion selective sensor in the circulating chloride solution.
6. The ion exchange was continuing until some kind of steady state was seen in the accumulated outflow of the exchanged ion.
7. If de-ionized water was going to be used as pore water in the drainage system during shearing, after the ion exchange, the chloride solution was exchanged for de-ionized water during the final days in the circulation system.
8. Finally, the specimens were dismantled and seven of the eight specimens were placed on top of each other to form a specimen with a height of 70 mm and a diameter of 35 mm, i.e. suitable for triaxial shearing.

Ion exchange to MX-80Ca

The chloride solution 0.1M $CaCl_2$ was chosen for the ion exchange of MX-80 to the calcium converted bentonite MX-80Ca. During the ion exchange, the potential (mV) of Na^+ was measured in the chloride solution after each change of solution. Figure A1-1 shows the concentration of Na^+, calculated from the measured potential and calibration of the sensor. Based on the calculated accumulated number of moles, shown in Figure A1-2, this circulation of chloride solution was terminated after 48 days (1,147 h). Before the dismantling de-ionized water was circulating during a couple of days since de-ionized water was to be used as pore water during shearing in the triaxial cell.

In Figures A1-3, A1-4, A1-5 and A1-6 corresponding results from the specimens MX-80Ca T2, MX-80Ca T3, MX-80Ca SP1 & SP2 and MX-80Ca SP3 & SP4 are shown.

Ion exchange to MX-80Na

The chloride solution 0.6 M NaCl was chosen for the ion exchange of MX-80 to the sodium converted bentonite MX-80Na. During the ion exchange, the potential (mV) of Ca^{2+} was measured in the chloride solution after each change of solution. Figure A1-7 shows the concentration of Ca^{2+}, calculated from the measured potential and calibration of the sensor. Based on the calculated accumulated number of moles, shown in Figure A1-8, the circulation of chloride solution was terminated after 76 days (1,820 h). At termination there was still an increase in the accumulated number of moles in the outflow. This was likely caused by a leakage of Ca^{2+} from slow dissolution of Calcite present in the MX-80. The leakage was assumed to be constant and continue for a long time. The chloride solution was kept as pore water during shearing in the triaxial cell.

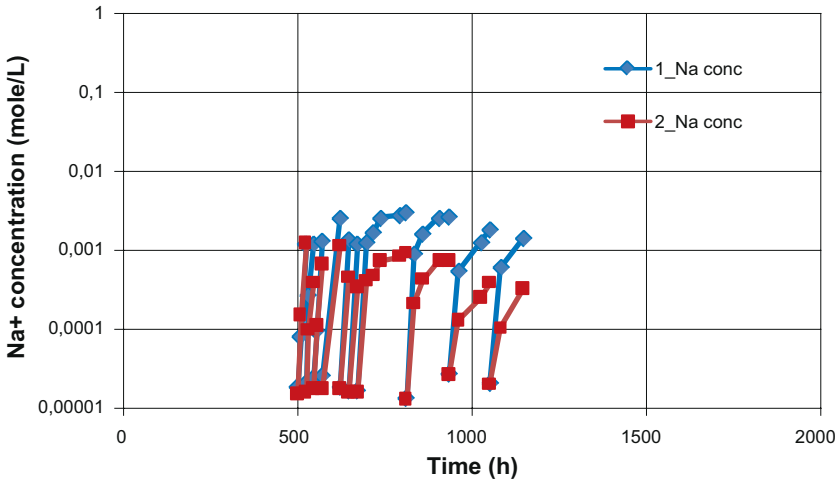

Figure A1-1. *Measured Na^+ concentration during the ion exchange to MX-80Ca. Results from the two devices 1 and 2 used for specimen MX-80Ca T1.*

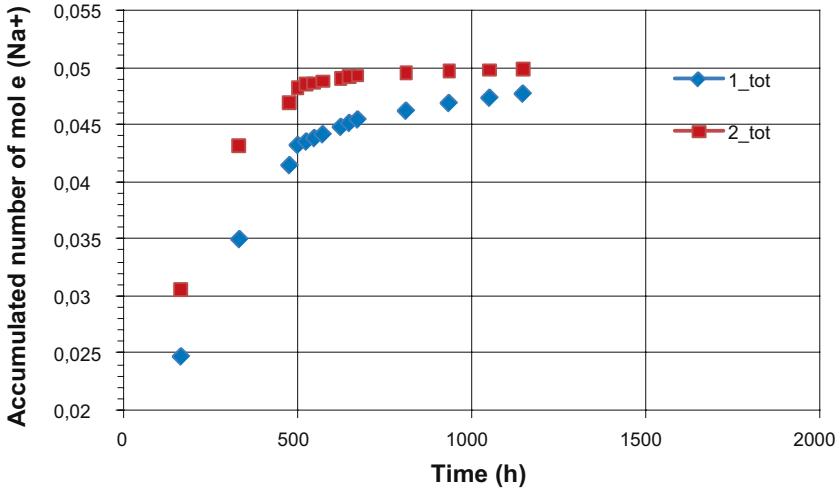

Figure A1-2. *Accumulated number of moles (Na^+) measured during the ion exchange to MX-80Ca. Results from the two devices1 and 2 used for specimen MX-80Ca T1.*

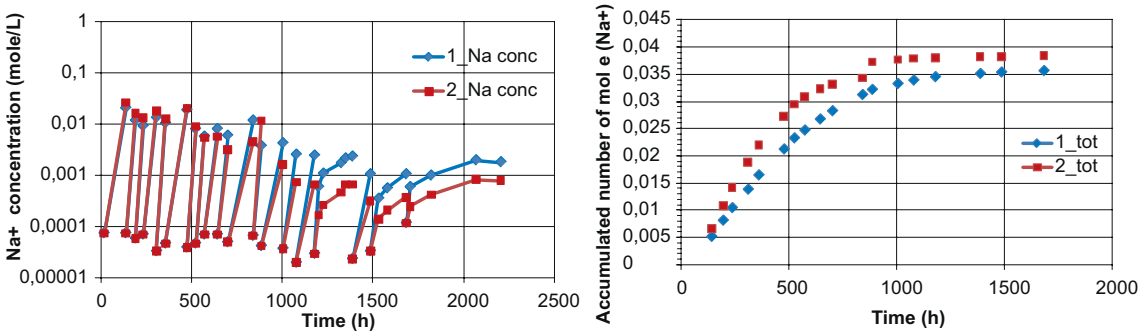

Figure A1-3. *Measured Na^+ concentration and calculated accumulated number of moles (Na^+) during the ion exchange to MX-80Ca for specimen MX-80Ca T2.*

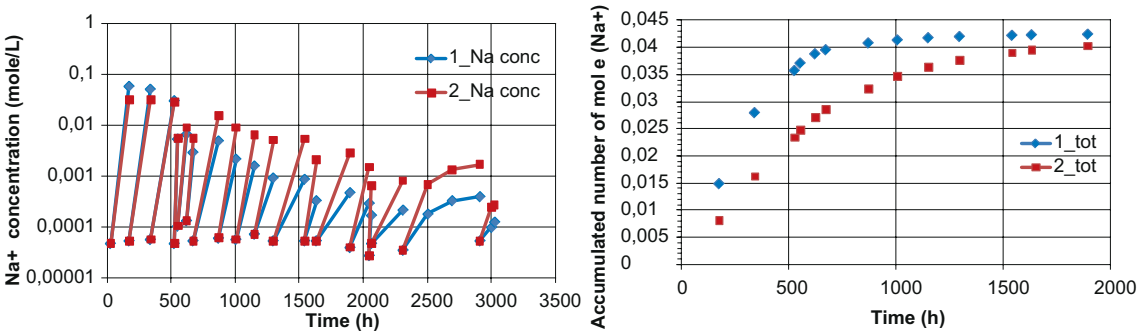

Figure A1-4. *Measured Na^+ concentration and calculated accumulated number of moles (Na^+) during the ion exchange to MX-80Ca for specimen MX-80Ca T3.*

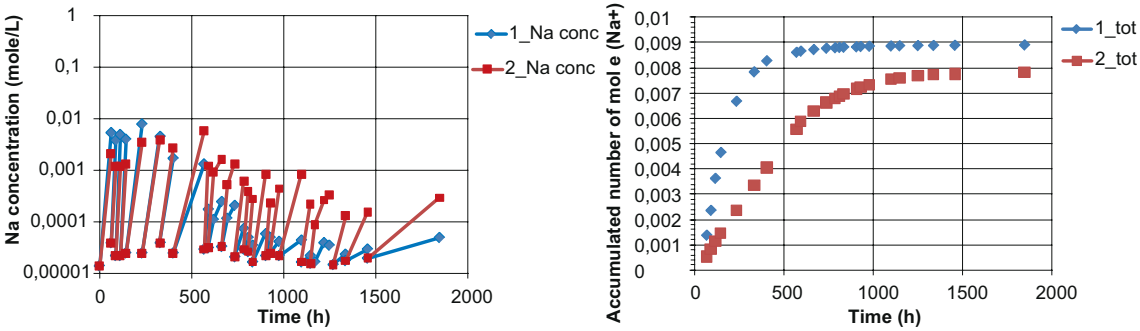

Figure A1-5. *Measured Na^+ concentration and calculated accumulated number of moles (Na^+) during the ion exchange to MX-80Ca for specimens MX-80CaSP1 and SP2.*

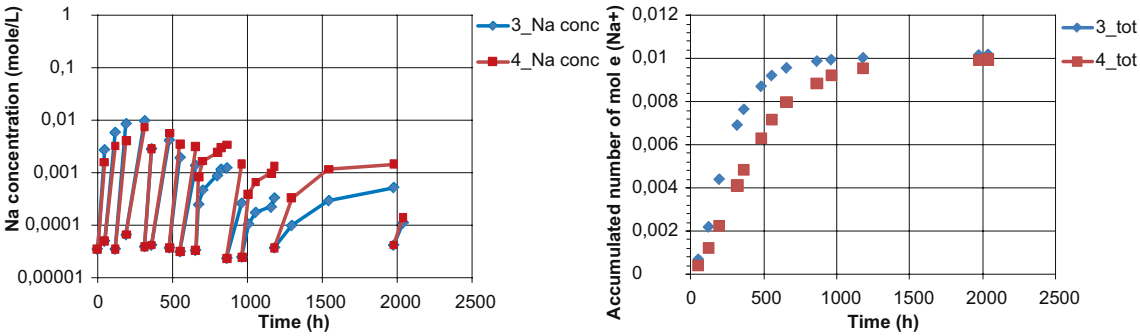

Figure A1-6. *Measured Na^+ concentration and calculated accumulated number of moles (Na^+) during the ion exchange to MX-80Ca for specimens MX-80CaSP3 and SP4.*

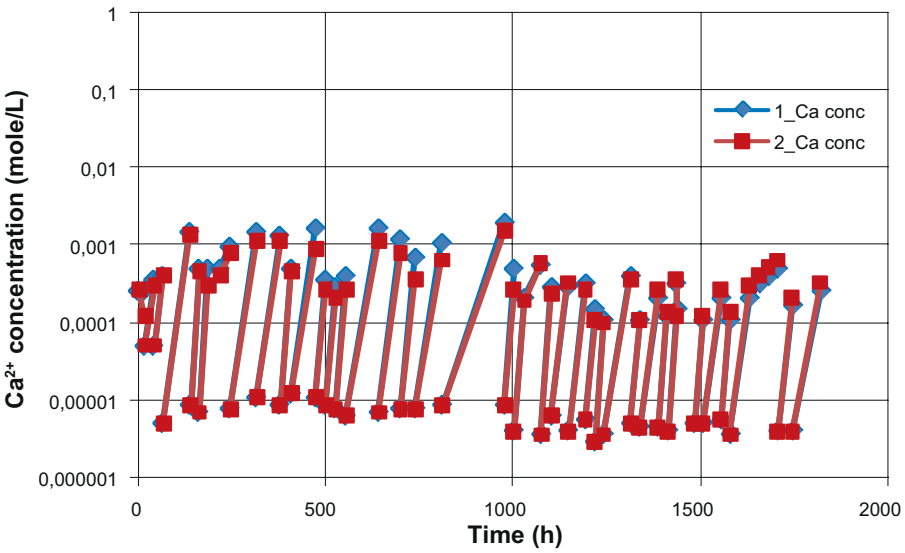

Figure A1-7. *Measured Ca^{2+} concentration during the ion exchange to MX-80Na. Results from the two devices 1 and 2 used.*

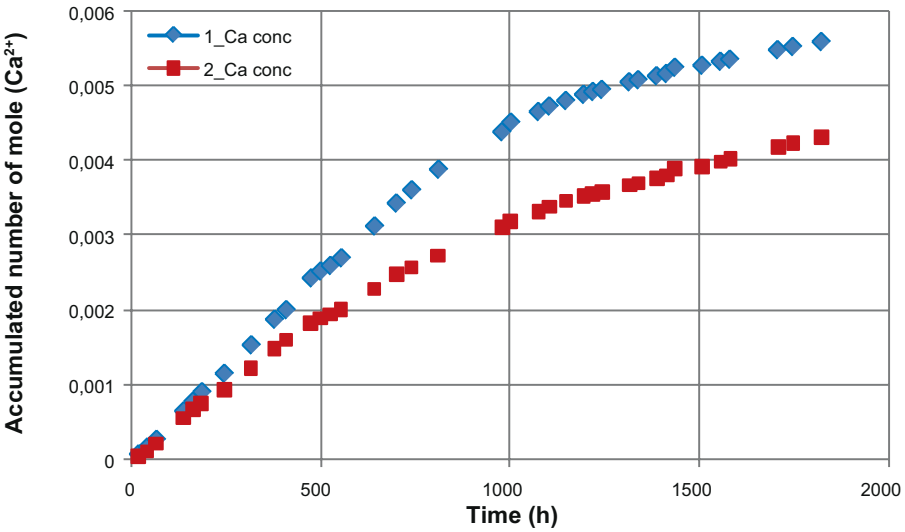

Figure A1-8. *Accumulated number of moles (Ca^{2+}) measured during the ion exchange to MX-80Na. Results from the two devices 1 and 2 used for MX-80Na T1.*

Results from triaxial tests

MX-80 T1 – Lab compacted

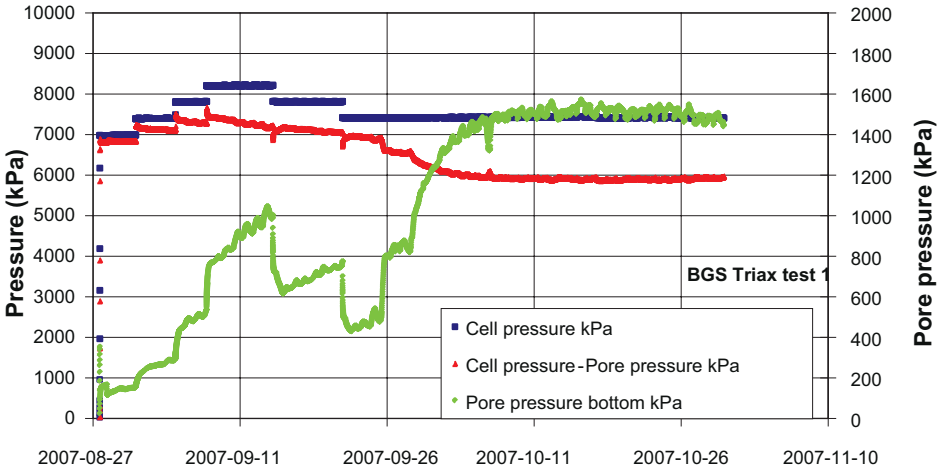

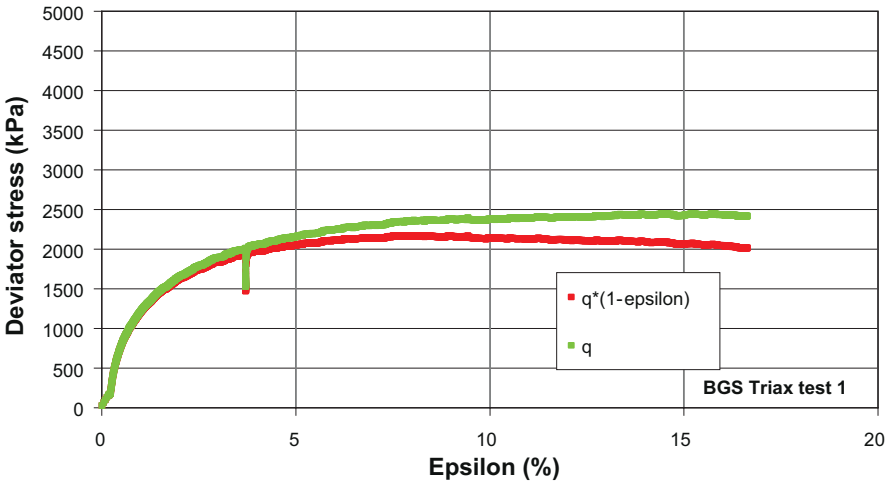

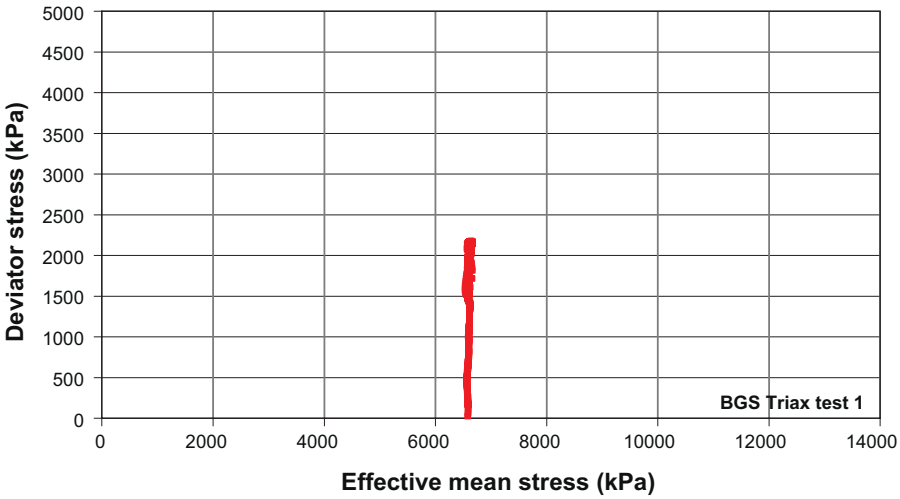

MX-80 T2 – Block before water pressure

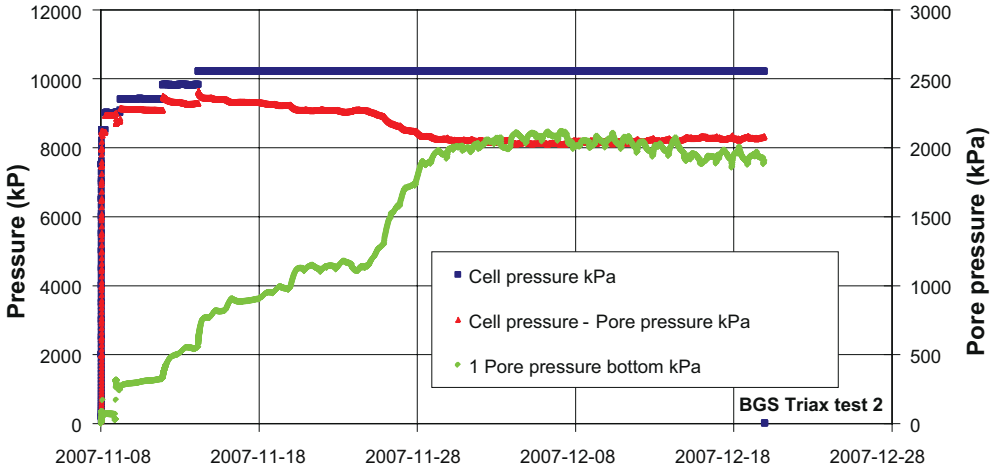

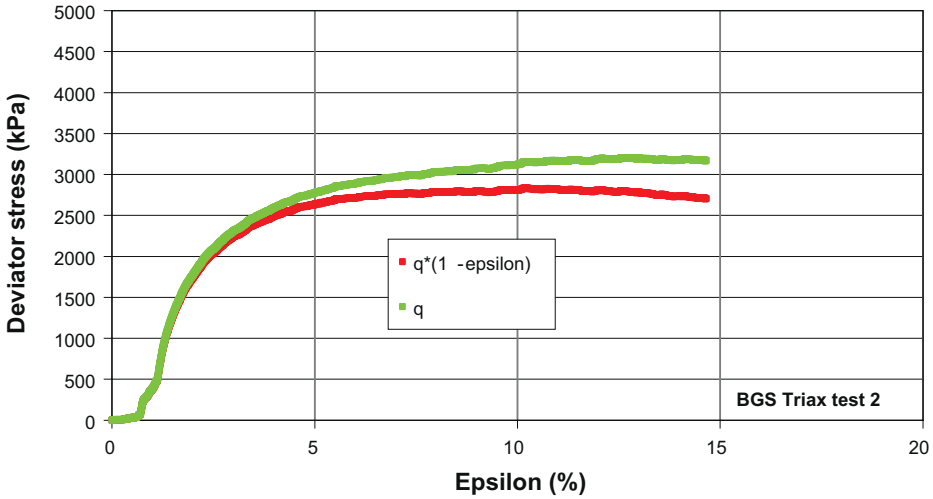

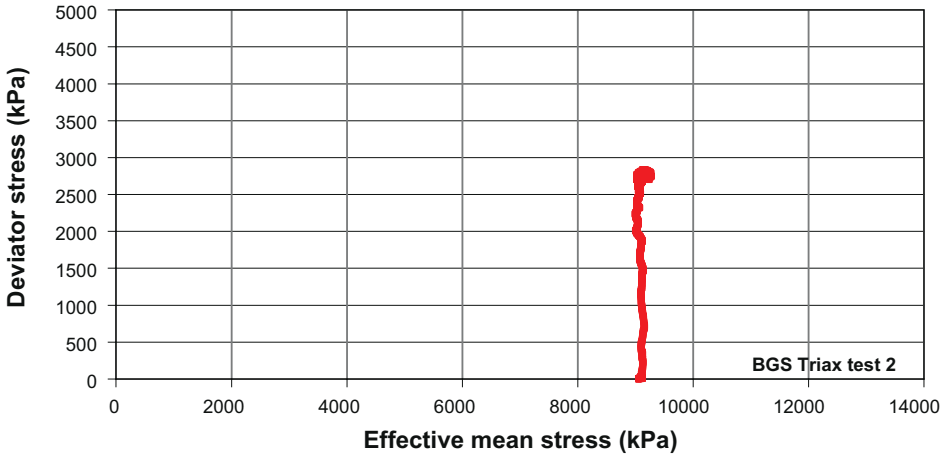

MX-80 T3 – Block after water pressure

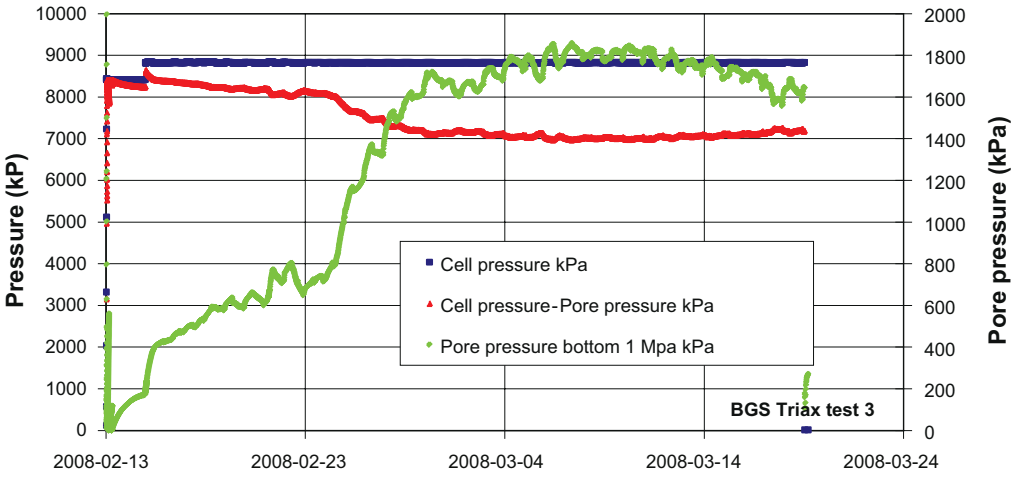

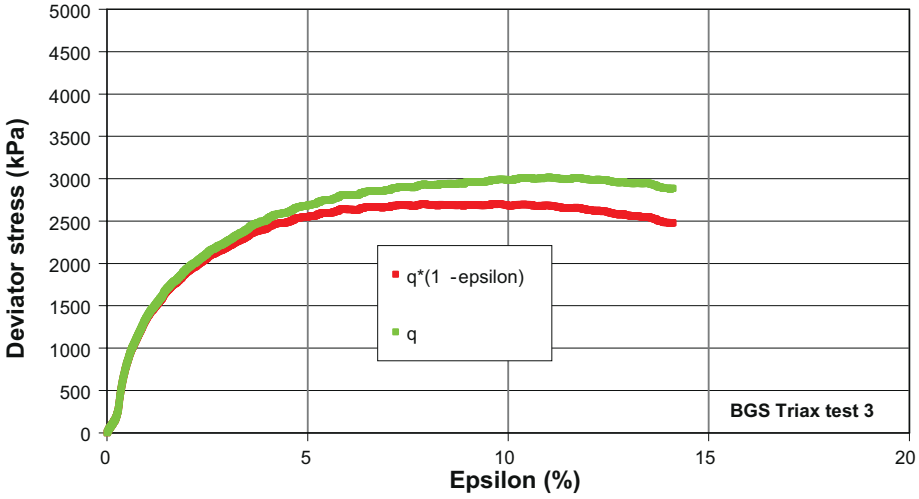

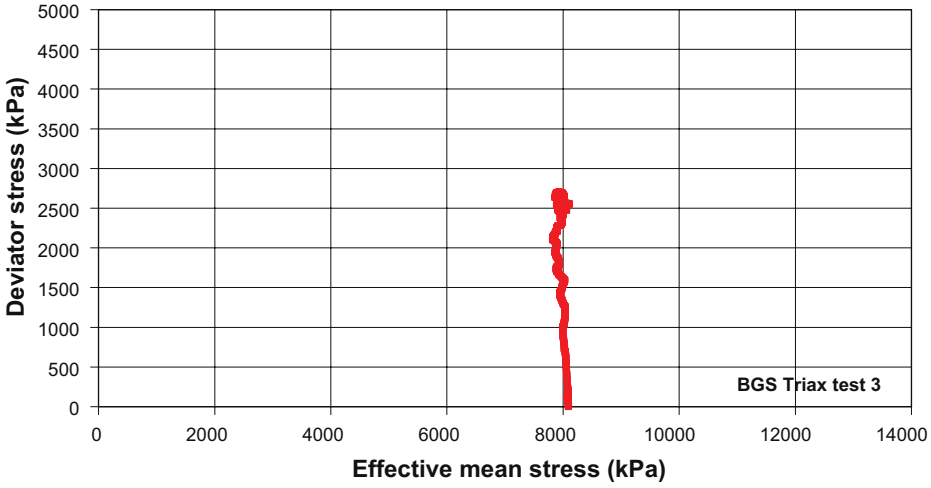

Deponit CaN – DepCaN T1

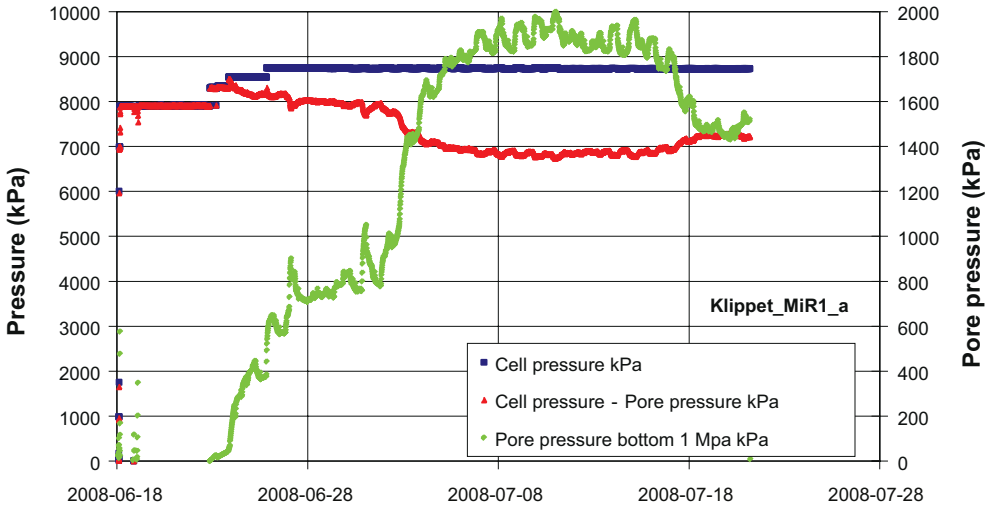

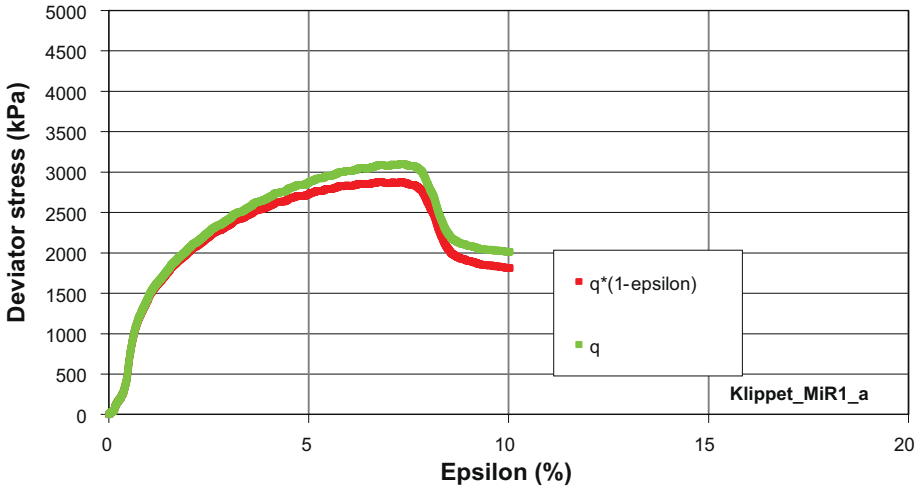

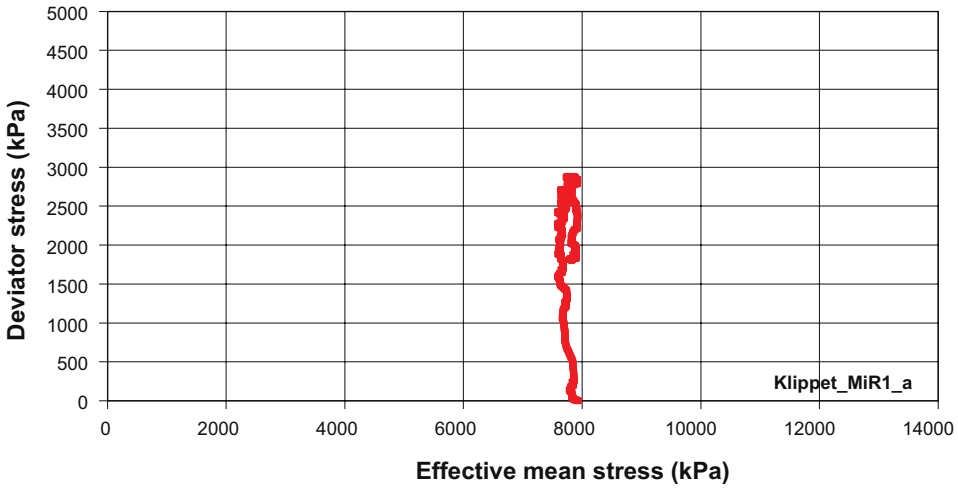

Deponit CaN – DepCaN T3

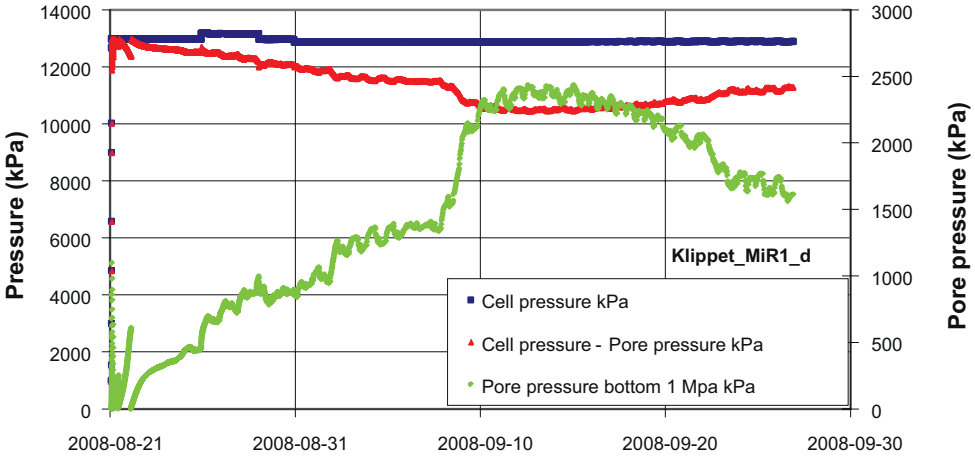

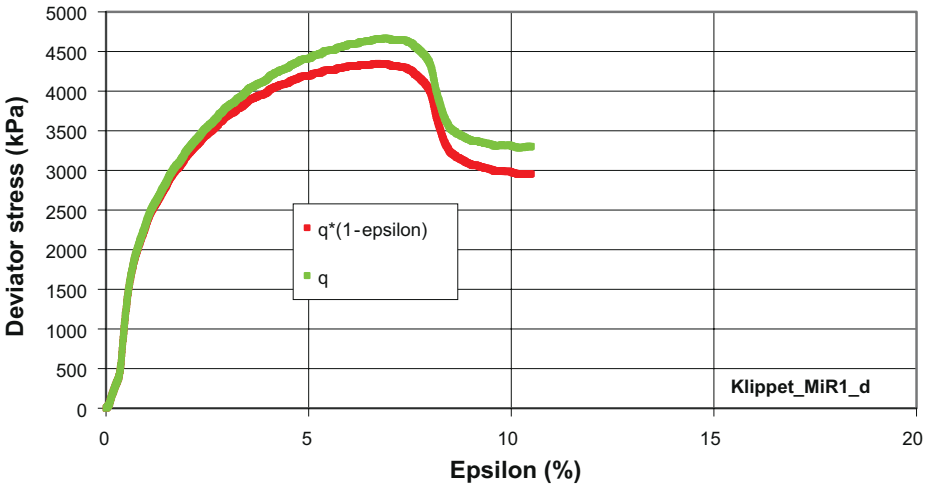

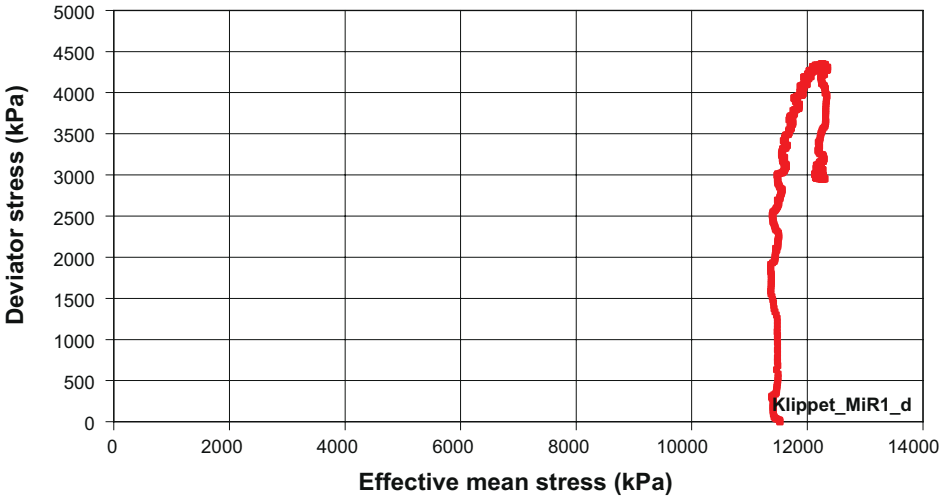

Ion exchanged MX-80: MX-80Ca T1

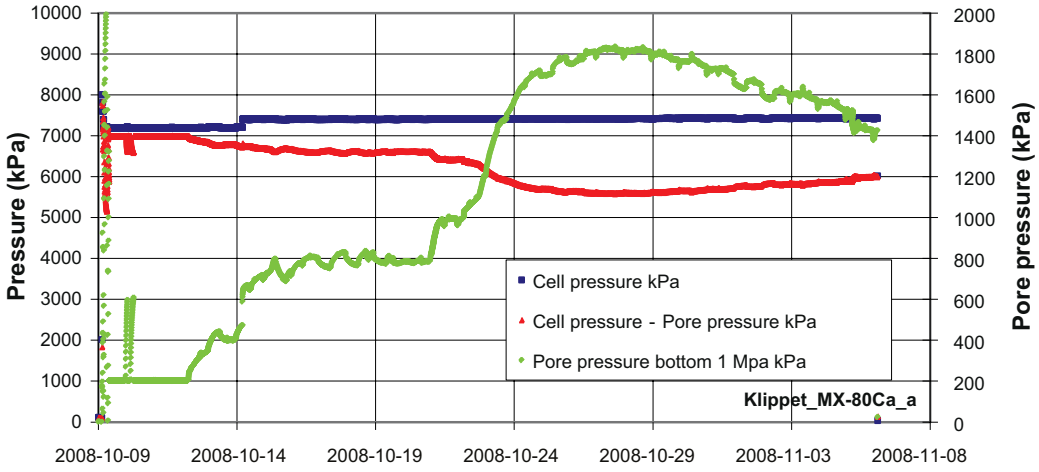

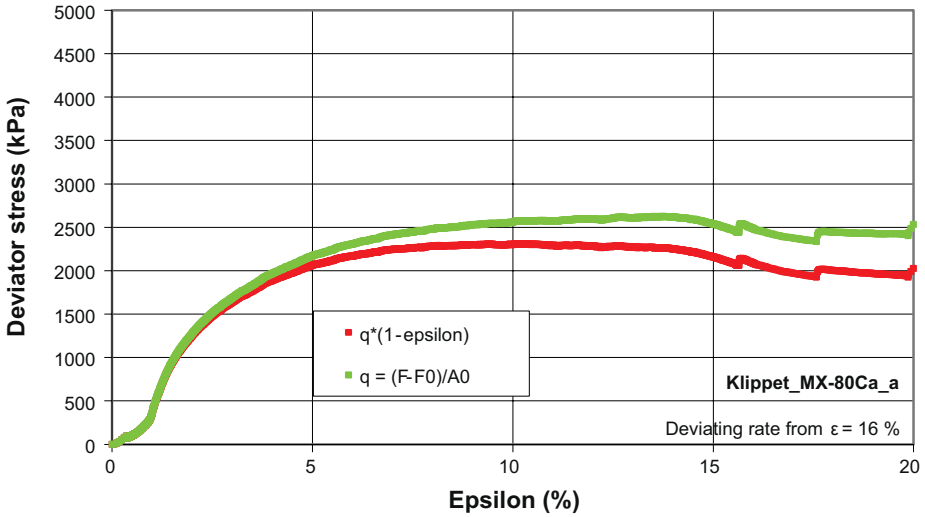

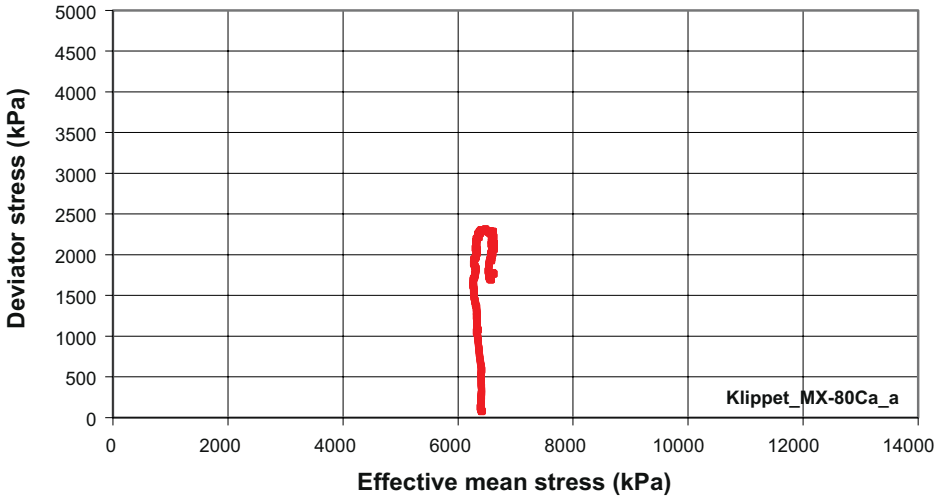

Ion exchanged MX-80: MX-80CaT2

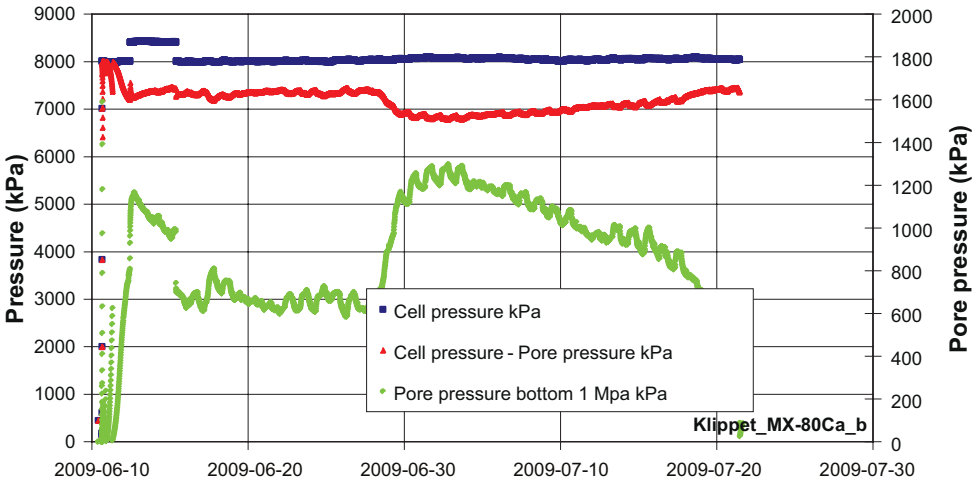

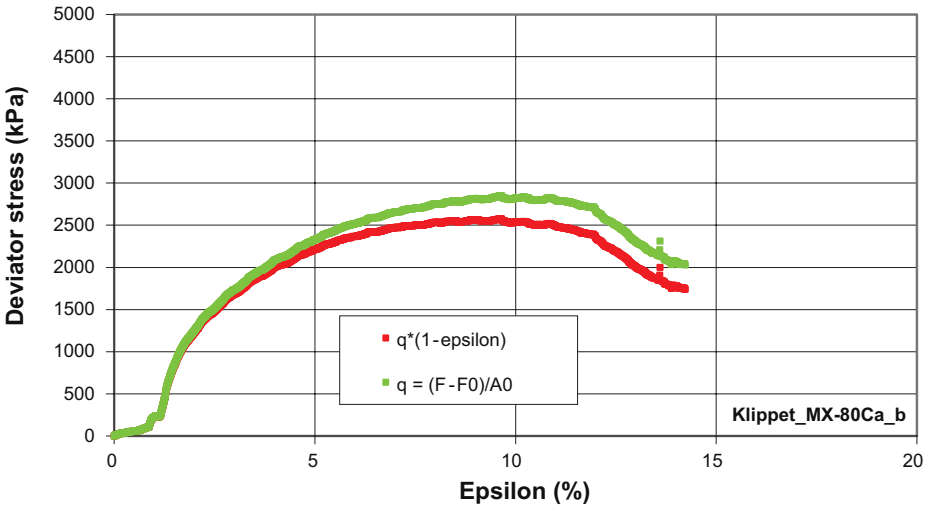

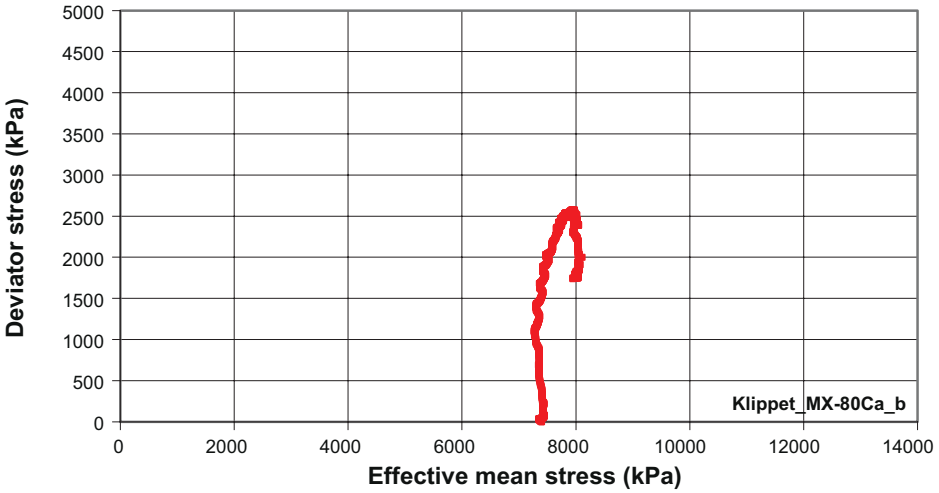

Ion exchanged MX-80: MX-80Ca T3

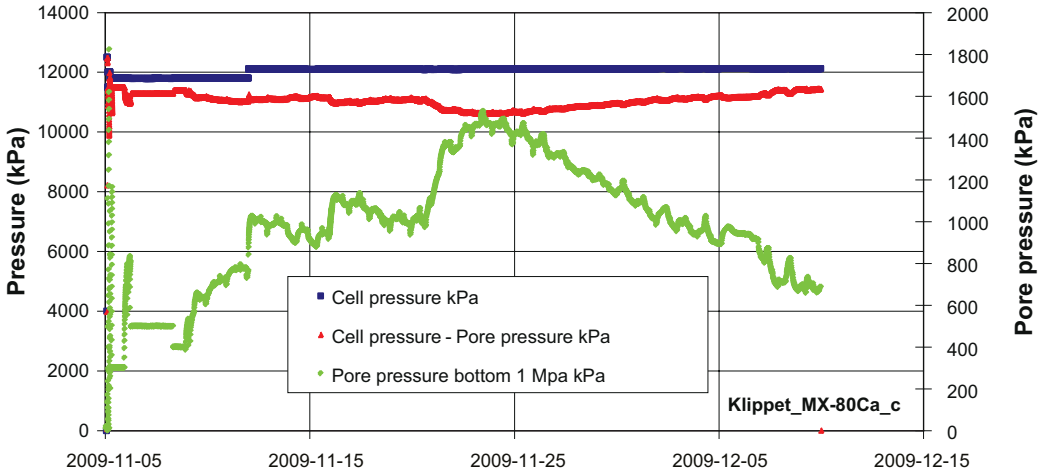

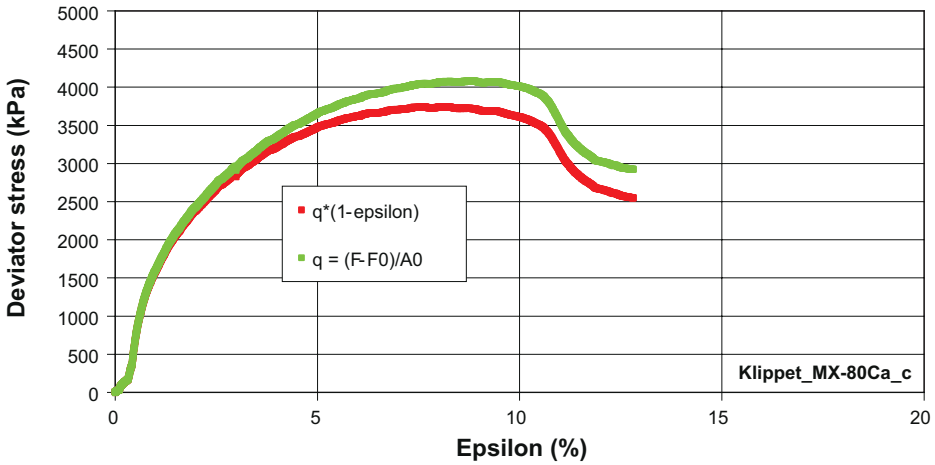

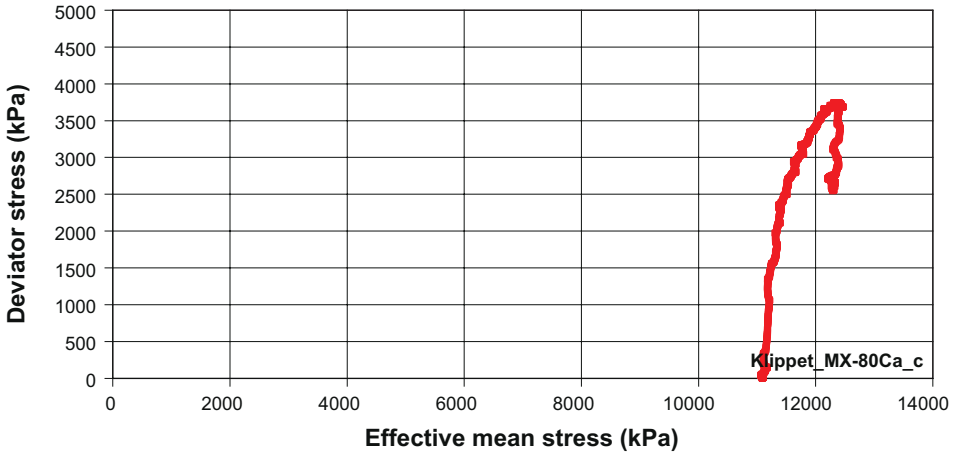

Ion exchanged MX-80: MX-80Na T1

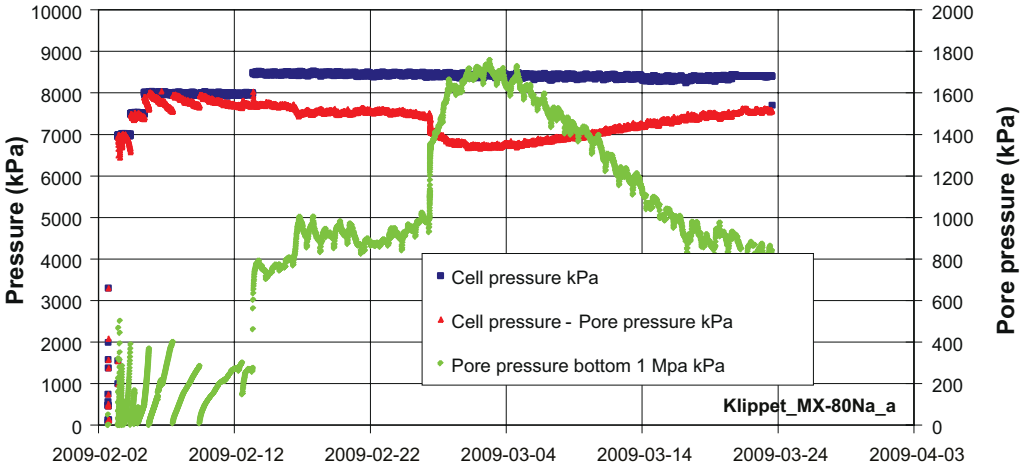

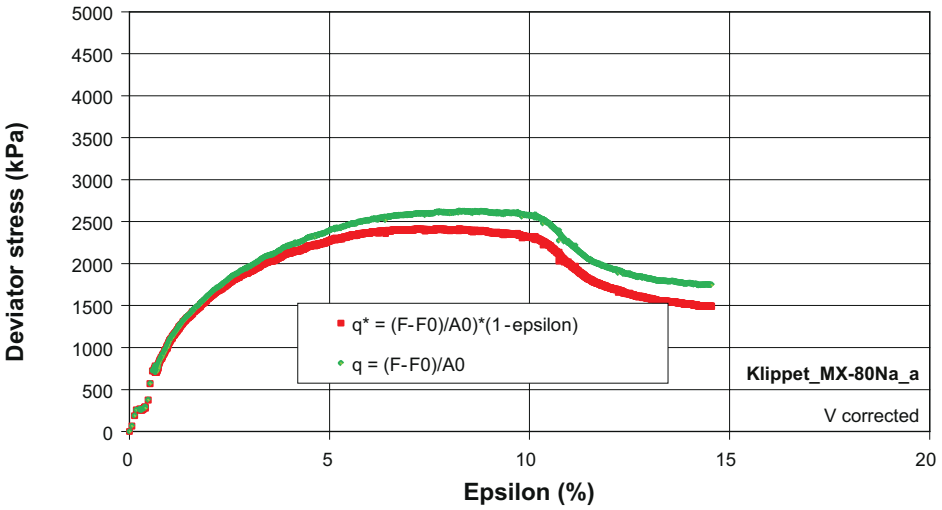

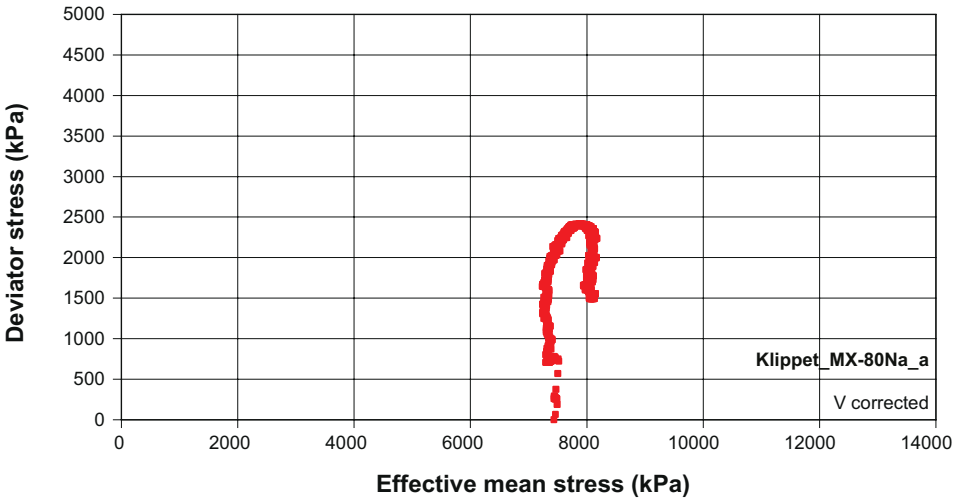

Appendix 3

Swelling during dismantling

Suppose that a core with less water content, higher density and lower void ratio was present and that these properties governed the measured mean stress during for example a triaxial test. Back-calculation from Equation 4-1 with the measured mean stress as swelling pressure gives a void ratio of 0.72 and the corresponding saturated water content is then 26%.

If a core with water content 26% and void ratio 0.72 was present the outer layer must have had a specific water content w_2 and specific void ratio e_2 to fit the measured average water content 28.5% and void ratio 0.79. Valid w_2 and e_2 for different thickness of the outer layer are shown in Figure A3-1. For example if the layer was 2.5 mm thick a water content of 35% and void ratio of 1 is necessary to get the measured average water content and void ratio.

From this it could not be excluded that the specimen MX-80 T2 had a core with less void ratio and less water content than the determined values show.

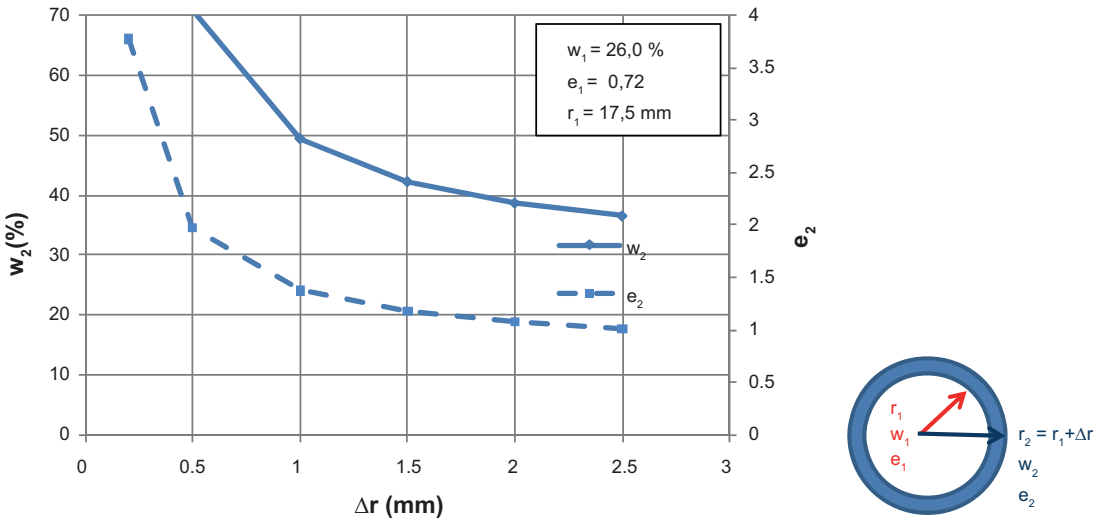

Figure A3-1. *Valid values of water content and void ratio for the outer layer vs. the thickness of the layer to fit the average values measured.*

Appendix 4

Triaxial tests with stress paths

The results from the triaxial tests in terms of deviator stress vs. effective average stress were given in Section 4.3 Shear strength. Below the same figure is given with the stress paths also shown for the tests conducted in this investigation.

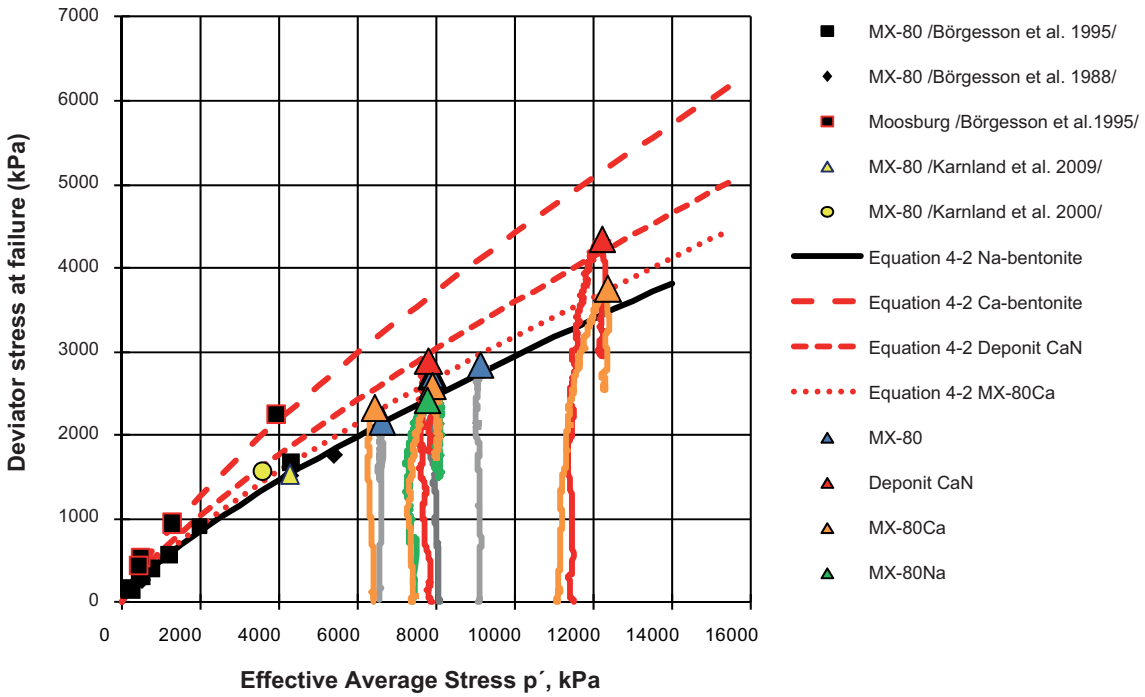

Figure A4-1. *Results from triaxial test series compared to test results from Karnland et al. (2000, 2009) (yellow) and Börgesson et al. (1988, 1995) (black). The almost vertical lines represent the measured stress paths during the shearing of the actual tests.*

Appendix 5

Shearing rate, results from MX-80Ca T1

The impact of rate on the deviator stress was investigated after the triaxial shearing of specimen MX-80Ca T1. The rates $9{\cdot}10^{-9}$, $9{\cdot}10^{-8}$, $9{\cdot}10^{-7}$ and $9{\cdot}10^{-6}$ m/s were used. Equation A5-1, which in its original form was presented by Börgesson et al. (2004), was used to correct for the different rates.

$$q_{corr} = q_{measured} \cdot \left(\frac{v_0}{v_{used}} \right)^n \qquad \text{(A5-1)}$$

where

q_{corr} corrected stress (kPa)

$q_{measured}$ measured stress (kPa)

v_0 = $9{\cdot}10^{-9}$ m/s

v_{used} = $9{\cdot}10^{-8}$, $9{\cdot}10^{-7}$ or $9{\cdot}10^{-6}$ m/s

n constant

The results are shown in Figures A5-1, A5-2 and A5-3 where the red lines represent the measured values. The green lines represent values corrected according to Equation A5-1 with the constant n equal to 0.065 and 0.022, respectively. The constant n equal to 0.065 was suggested for MX-80 by Börgesson et al. (2004).

The result indicates that if the constant n equals 0.065, as suggested for MX-80 by Börgesson et al. (2004), the influence of deformation rate seems to be too strong for rates from $1{\cdot}10^{-8}$ to $1{\cdot}10^{-5}$ m/s. It should be noted that the change in rate was done in the slow range of deformation rates and it is possible that the result is not fully representative for the high range. It should also be mentioned that the change in rate started late in the shearing process (after 15% strain) and that the material used was not MX-80 but the ion exchanged material MX-80Ca.

Figure A5-4 shows the ratio between the measured and the corrected deviator stress, i.e. the ratio between the red and green lines from Figure A5-3, vs. the rate.

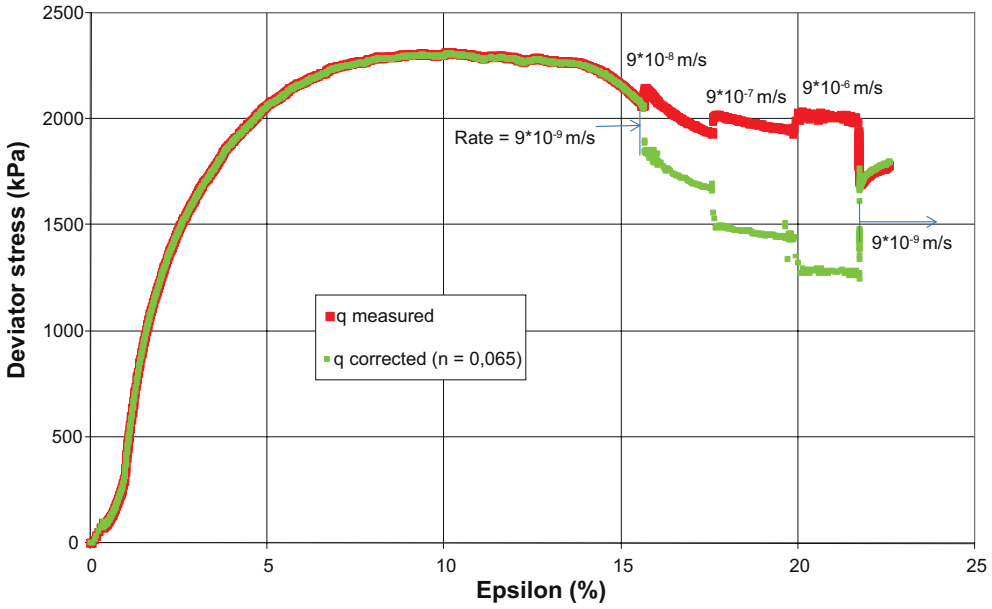

Figure A5-1. *Results from specimen MX-80Ca T1 and the study of influence of rate on stress. The red and green lines represent measured and corrected values, respectively. For the corrected values the constant n, Equation A5-1, equals 0.065.*

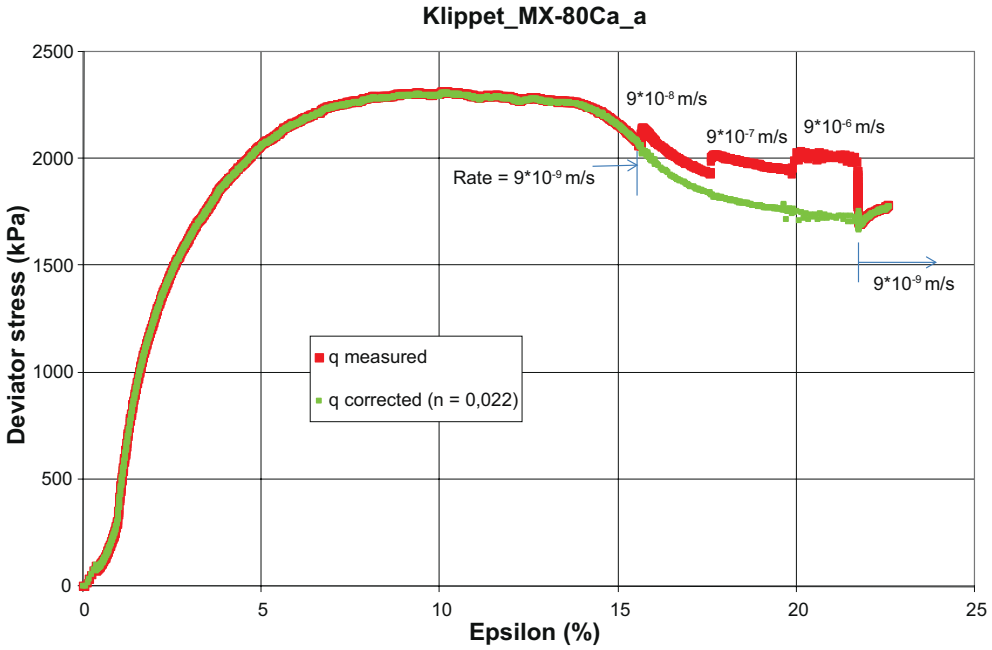

Figure A5-2. *Results from specimen MX-80Ca and the study of influence of rate on stress. The red and green lines represent measured and corrected values, respectively. For the corrected values the constant n, Equation A5-1, equals 0.022.*

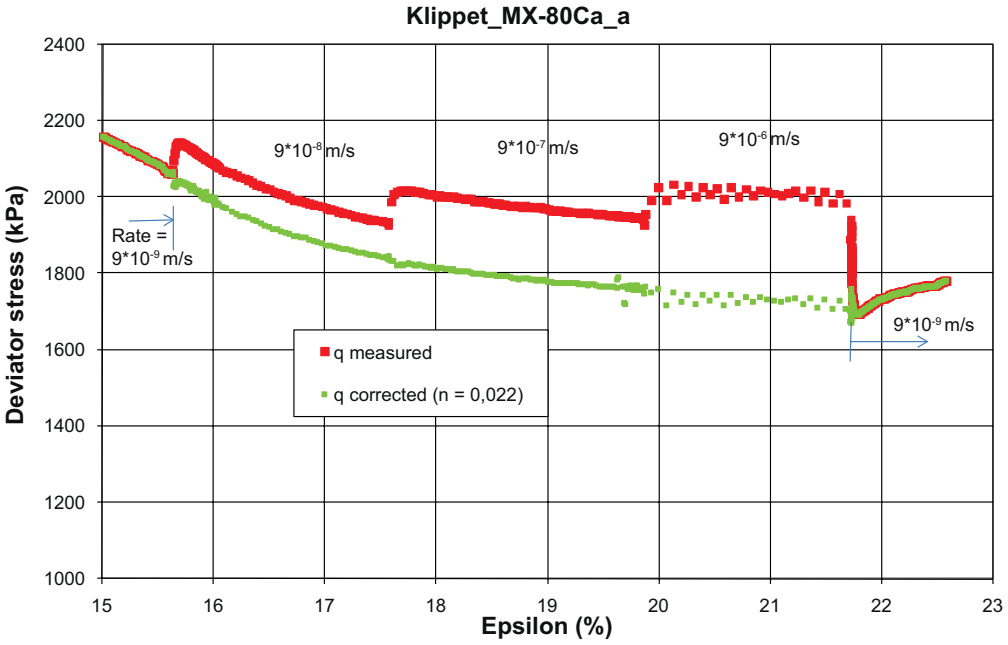

Figure A5-3. *The final part of Figure A5-2.*

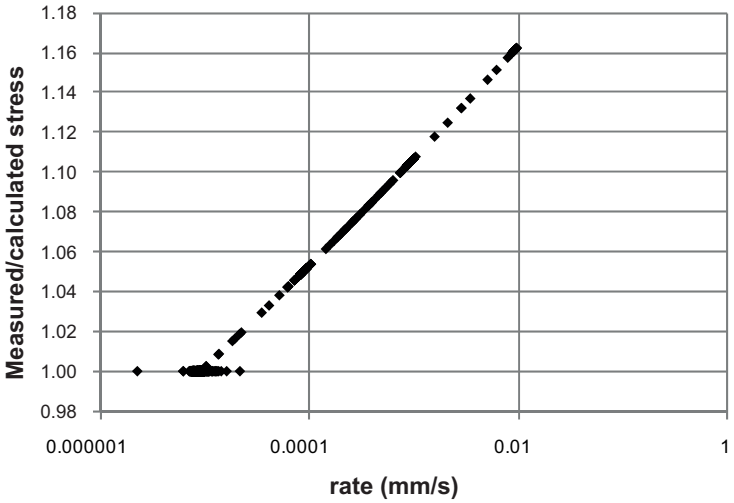

Figure A5-4. *The ratio between the measured (not corrected) and corrected deviator stress in Figure A5-3 plotted vs. the rate used.*

Appendix 6

Unconfined compression tests at 12˚C, temperature measurements

Unconfined compression tests were carried out at lower temperature than the room climate, approximately 21˚C. The purpose was originally to determine the deviator stress during shearing at 5˚C.

For this purpose specimens were saturated during 14 days at 5˚C in a controlled refrigerator. After dismantling the specimens were stored at 5˚C for 12h until the shearing.

The shearing was carried out with the ordinary mechanical press used for this type of shearing. An insulated box was manufactured to enclose the specimen and the upper part of the base pedestal (cf. Figure 2-2). In a reference test the temperature in the insulated box was measured with two thermocouples and the results are shown in Figure A6-1. The laboratory room temperature is also shown in this figure. The events (1) to (4) refer to the procedure used.

Before the shearing ice packs were placed inside the box to keep the temperature low (1). One of the thermocouples was then placed inside the specimen in a 5 mm deep, drilled hole (2). The box was sealed (3) and was after 15 minutes, the time period for an ordinary test, opened again (4).

During an ordinary testing time the temperature increased from approximately 8˚C to 14˚C inside the specimen. In the test results 12˚C is used as the average and approximate temperature for these specimens.

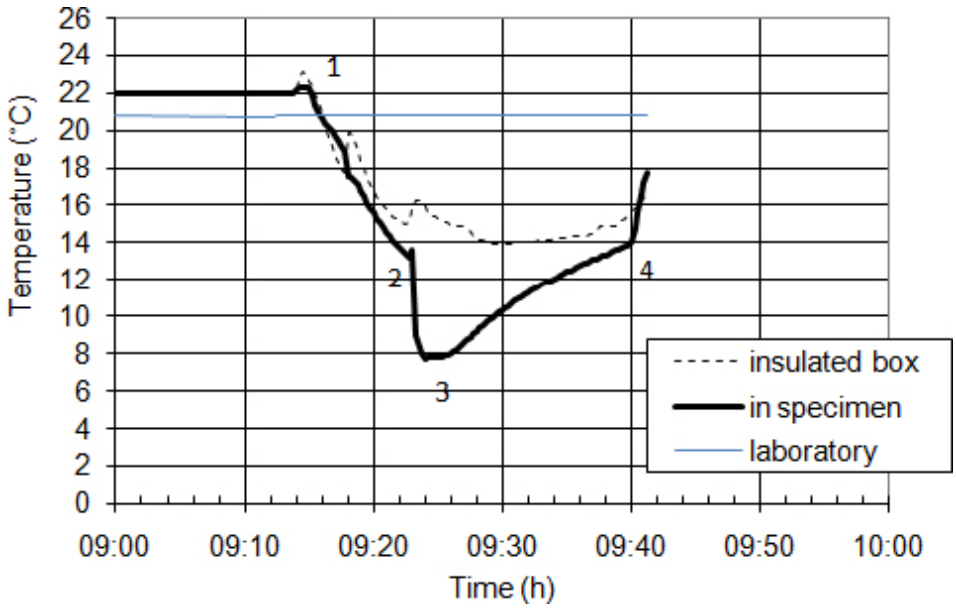

Figure A6-1. *Measured temperature with one thermocouple inside the insulated box and one mounted inside the specimen. Events (1) to (4) refer to the procedure.*

Appendix 7

Fast shearing, results in tables

Table A7-1. Results from unconfined compression tests at different rates on MX-80.

Material	Name	Measurements					Constants		Calculated	
			Strength		Base variables					
		rate mm/s	q_{max} kPa	strain %	ρ^1 kg/m³	w^1 %	ρ_s kg/m³	ρ_w kg/m³	e	S_r %
MX-80	D01	0.003	3,803	5.8	2,050	23.8	2,780	1,000	0.68	97
	D02	0.1	3,909	5.4	2,040	24.5	2,780	1,000	0.70	97
	D03	10	4,094	5.3	2,030	24.7	2,780	1,000	0.71	97
	D04	98	4,391	5.7	2,030	24.9	2,780	1,000	0.71	97
	D05	268	4,979	5.4	2,030	24.4	2,780	1,000	0.70	97
	D06	271	5,136	5.9	2,040	24.1	2,780	1,000	0.69	97
MX-80 pre	DT1	192	6,171	4.4	2,080	22.2	2,780	1,000	0.63	98
	DT2	218	6,978	4.9	2,070	22.2	2,780	1,000	0.64	96

[1] average of two specimens

Table A7-2. Results from unconfined compression tests at different rates on Deponit CaN.

Material	Name	Measurements					Constants		Calculated	
			Strength		Base variables					
		rate mm/s	q_{max} kPa	strain %	ρ^1 kg/m³	w^1 %	ρ_s kg/m³	ρ_w kg/m³	e	S_r %
DepCaN	E01	0.003	4,959	3.1	2,060	23.7	2,750	1,000	0.65	101
	E02	0.003	4,837	4.5	2,050	24.1	2,750	1,000	0.66	100
	E03	0.1	5,091	3.3	2,040	24.5	2,750	1,000	0.68	100
	E04	1	5,685	4.3	2,050	25.1	2,750	1,000	0.68	102
	E05	10	6,551	4.3	2,050	24.5	2,750	1,000	0.67	101
	E06	98	6,841	5.0	2,050	25.0	2,750	1,000	0.68	102
	E07	218	6,607	5.7	2,050	24.9	2,750	1,000	0.68	101
	E08	269	6,631	5.4	2,040	24.9	2,750	1,000	0.68	100
	E09	0.1	5,405	3.3	2,050	24.5	2,750	1,000	0.67	101
	E10	1	6,239	3.3	2,060	24.1	2,750	1,000	0.66	101
	E11	10	6,245	4.4	2,060	24.3	2,750	1,000	0.66	101
	E12	97	6,578	5.1	2,050	24.5	2,750	1,000	0.67	101
	E13	275	6,800	5.1	2,050	24.6	2,750	1,000	0.67	101
	E14	266	7,409	4.7	2,050	24.2	2,750	1,000	0.66	100
DepCaN pre	ET1	105	8,268	3.5	2,070	22.1	2,750	1,000	0.62	97
	ET2	0.1	6,456	2.5	2,070	22.0	2,750	1,000	0.62	97
	ET3	226	7,852	3.9	2,060	22.5	2,750	1,000	0.64	97
	ESP1	239	8,693	4.4	2,070	22.6	2,750	1,000	0.63	99
	ESP2	236	9,169	4.2	2,070	22.8	2,750	1,000	0.63	100

[1] average of two specimens

Different preparations were used for the specimens. The specimens D1–D6 and E1–E14 were compacted and then saturated in a saturation device. The specimens DT1, DT2 and ET1–ET3 were compacted from high water content, between 23% and 27%, to almost full saturation. Specimens ESP1 and ESP2 were drilled from a saturated specimens from the swelling pressure device.

Appendix 8

Test matrix

In Table A8-1 the number of tests for each material used is noted.

Three types of bentonite were tested; MX-80, Deponit CaN and ion exchanged MX-80, denominated MX-80Ca and MX-80Na. The third type of bentonite included in this present study is the ion exchanged MX-80, which was prepared according to Appendix 1. In addition purified materials, WyCa and WyNa, were used in one test series to study the difference in behaviour between sodium and calcium bentonite. These purified materials were ion exchanged from MX-80 according to Karnland et al. (2006) and all accessory minerals were removed.

Swelling pressure was only measured on one Deponit CaN specimen according to the description in Section 2.5. However, the Deponit CaN specimens used for the triaxial tests having a height of 70 mm and a diameter of 35 mm were saturated in a device where swelling pressure was measured in a slightly different way. In addition to the two triaxial tests on Deponit CaN a third specimen of Deponit CaN was saturated in this device and resulting in an additional measured swelling pressure. However, this specimen was not mounted into the triaxial cell. Thus, swelling pressure on Deponit Can was measured on four specimens, cf. Figure 3-7, but only one swelling pressure test was carried out according to Section 2.5.

Table A8-1. Test matrix for the materials used.

Test type	Abbr.	MX-80	Deponit CaN	MX-80Ca MX-80Na	Purified MX-80
Swelling pressure test	SP	2	1	4	
Triaxial test	T	3	2[1]	4	
Unconfined compression test	UC	5	6		6
Unconfined compression test (fast)	UC	8	19		

[1] A special measurement of swelling pressure was made.